BMI-1554

PROGRESS IN THE DEVELOPMENT OF URANIUM CARBIDE-TYPE FUELS

Final Report on the AEC Fuel-Cycle Program

BATTELLE MEMORIAL INSTITUTE

Printed in USA
Price $1.50

Available from the
Office of Technical Services
U. S. Department of Commerce
Washington 25, D. C.

Report No. BMI-1554

UC-25 Metals, Ceramics, and Materials
(TID-4500, 16th Ed.)

Contract No. W-7405-eng-92

PROGRESS ON THE DEVELOPMENT OF URANIUM CARBIDE-TYPE FUELS

Final Report on the
AEC Fuel-Cycle Program

Edited by

Frank A. Rough
Walston Chubb

Work done by

Alfred E. Austin
Burton C. Boesser
Walston Chubb
Norman E. Daniel
Roy W. Endebrock
Ellis L. Foster
David G. Freas
John E. Gates
Ralph W. Getz
Carl W. Melton
Charles W. Townley

November 17, 1961

BATTELLE MEMORIAL INSTITUTE
505 King Avenue
Columbus 1, Ohio

TABLE OF CONTENTS

PROGRESS ON THE DEVELOPMENT OF URANIUM CARBIDE-TYPE FUEL MATERIALS

Final Report on AEC Fuel-Cycle Program

Edited by Frank A. Rough and Walston Chubb

A 2-1/2-year study of uranium monocarbide under the AEC Fuel-Cycle Development Program, discussed in BMI-1370 and BMI-1488, has been concluded. The skull arc-melting equipment and process have been developed to produce 6-kg castings with a carbon content predictable within ± 0.05 w/o. The preparation of a homogeneous skull is one of the most important factors in obtaining this control, and may be accomplished by melting prealloyed uranium carbide in a water-cooled copper crucible. Once a homogeneous skull has been prepared, this compositional control can be maintained even with elemental charges. Erosion of the graphite electrode is minimized by using outgassed TSF graphite and is compensated for by adding small amounts of elemental uranium. The highest quality material is produced by vacuum melting and casting procedures. Hot hardness, dilation, and resistivity measurements to about 1600 C were performed. A change in state of UC_2 at about 870 C was indicated. As-cast mixtures of UC and UC_2 containing 7.0 w/o carbon were found to transform to U_2C_3 on reheating by a sluggish reaction between 1100 and 1700 C. Rates of self-diffusion of carbon in uranium monocarbide were about 1000 times the rates of self-diffusion of uranium in uranium monocarbide between 1200 and 2200 C. Below 700 C, uranium monocarbide showed no gross dimensional changes as a function of irradiation to a burnup of 0.7 a/o of the uranium. Resistivity and lattice strain of uranium monocarbide showed significant changes at a burnup of only 0.004 a/o of the uranium. No further significant change occurred as a function of additional burnup. A portion of this effect was annealed out in irradiation at 700 C. Uranium sesquicarbide showed no gross dimensional changes under irradiation to a burnup of 0.56 a/o of the uranium at about 700 C. Metastable uranium dicarbide structures which had begun to precipitate graphite were not compatible with NaK.

INTRODUCTION

The research discussed in this report was sponsored by the Reactor Development Division of the U. S. Atomic Energy Commission as part of the Fuel-Cycle Development Program and constituted a portion of an effort to evaluate and develop uranium monocarbide as a fuel for nuclear power reactors. Because of its high density and refractory, submetallic nature, uranium monocarbide presented considerable promise as a power reactor fuel at the outset of this program. At the conclusion of this program it can be stated that there is no reason to suppose that this expectation cannot be realized.

For purposes of administration and reporting, this program of research was divided into three temporal periods and into five subjective divisions. The three temporal periods consisted of 6 months, 1 year, and 1 year in consecutive order beginning April 1, 1959. This report covers the research performed in the third period (12 months long), designated Phase III. The five subjective divisions or areas of research were:

(1) An investigation of reactions and techniques by which uranium carbide powder can be synthesized and consolidated into dense bodies without resorting to melting and casting. The final report on these studies was included in the Phase II report, BMI-1488, December 27, 1960.

(2) Development of equipment and techniques for melting and casting of uranium carbide shapes of reproducible dimensions, soundness, and analysis. Research during Phase III has been devoted primarily to developing specifications for preparing large ingots of controlled and reproducible carbon content.

(3) Determination of the physical, mechanical, and chemical properties of uranium carbides. The major effort in this area during the last year has been the determination of mechanical and physical properties at temperatures up to 1600 C.

(4) Measurement of the rates of interdiffusion and self-diffusion of uranium and carbon in uranium carbides. This research was concluded before the end of Phase III and the results were discussed in detail in a separate report.(1)

(5) Studies of the processes and mechanisms leading to damage in uranium carbide as a result of reactor irradiation. These studies have involved physical-property measurements of samples irradiated to various burnups up to 0.7 a/o of the uranium at temperatures below about 980 C.

All efforts in the four areas of research above which were active during Phase III of the Fuel-Cycle Development Program have now been concluded. This report constitutes the final report on research in the areas of melting and casting, mechanical and physical properties, and mechanisms of irradiation damage in uranium carbide.

MELTING AND CASTING OF UC

Uranium monocarbide is an attractive nuclear fuel because of its high density and good thermal conductivity as compared to other uranium compounds. To fully exploit these properties it is desirable that the fabrication techniques employed in its production yield a dense product free of interfaces or voids that might lower its density or thermal conductivity. Casting techniques can yield a product which is essentially 100 per cent dense. For this reason melting and casting appeared to be a promising method of producing uranium-carbon alloys in shapes suitable for use as reactor fuels at the start of the present work under the AEC Fuel-Cycle Development Program.

Laboratory techniques capable of producing stoichiometric uranium monocarbide shapes had been developed previously.(2) These techniques were further developed in the present program until it was possible to produce small cylindrical shapes of uranium-carbon alloys over a wide composition range with excellent compositional control, i.e., ±0.15 w/o carbon. However, these laboratory techniques were not

(1) References at end.

directly amenable to scale-up or automation and, therefore, did not appear attractive as economical methods for the quantity production of fuel elements. A more satisfactory technique for the production of large quantities of cast UC shapes was desired, and an investigation of inert-electrode skull-type arc-melting techniques was initiated.

The results obtained during the initial studies of skull-type arc melting for the production of uranium carbide shapes were reported in BMI-1488.[3] During these studies this melting technique was shown to be a practical method for production of large shapes of UC suitable for fuel elements. It was demonstrated that various shapes and configurations could be cast with good surface quality and dimensional tolerances. The desirability of using heated molds was demonstrated by the improved soundness and surface condition exhibited by castings poured into molds of this type under a dynamic vacuum. A major problem of the skull-melting technique was found to be control of the composition of uranium-carbon alloys. Two or more castings poured simultaneously from a single melt exhibited variations in carbon content of less than 0.1 w/o. However, castings poured at different times utilizing the same skull exhibited carbon variations up to and sometimes in excess of ±0.3 w/o. This variation in carbon content was attributed to the irregular rate of introduction of carbon into the melt by erosion of the graphite-tipped electrode. As a consequence, the factors which influence the composition of skull-melted UC castings were investigated as part of the final phase of this program.

Experimental Equipment

The basic features of the skull-melting apparatus initially used and its auxiliary power source were discussed in BMI-1488.[3] This furnace and various sizes of water-cooled copper crucibles were used for the major portion of these studies. However, during the latter part of the program, alterations were made in the furnace to permit control of composition by adding materials during melting. Changes in the design of the electrode also were made to permit the use of readily available shapes of graphite.

The furnace alterations consisted of the addition of a hopper and feed mechanism to the vacuum shell to permit the addition of elemental uranium and carbon during the melting cycle. A schematic of the furnace and feed mechanism is shown in Figure 1. The charge control and feed mechanism, A, E, and D, were used to introduce up to 14 additions of elemental materials of predetermined composition into the crucible. The concentric-tube assembly and feed trough, F, G, and L, were necessary to permit the accurate placement of the feed trough when melting and the retraction of this trough when pouring. The ball joint, K, provided a vacuumtight seal while facilitating lateral movement of the trough. Since the trough had to be retracted prior to pouring, the feed trough was welded to the tube, F, which permitted the use of O-ring seals to maintain a reduced pressure in the furnace. The other features of the furnace modifications are shown in the schematic. This arrangement permitted the operator to add either uranium or carbon to the crucible either in predetermined amounts or as dictated by the erosion of the graphite electrode. The valving between the mechanism and the furnace chamber permits isolation of the feed-mechanism system from the furnace chamber so that new charges may be added to the hopper and eventually to the crucible without disturbing the atmosphere surrounding the skull. Thus, large amounts of new material may be added to the molten pool without cooling highly reactive materials and opening the furnace each time an addition was made.

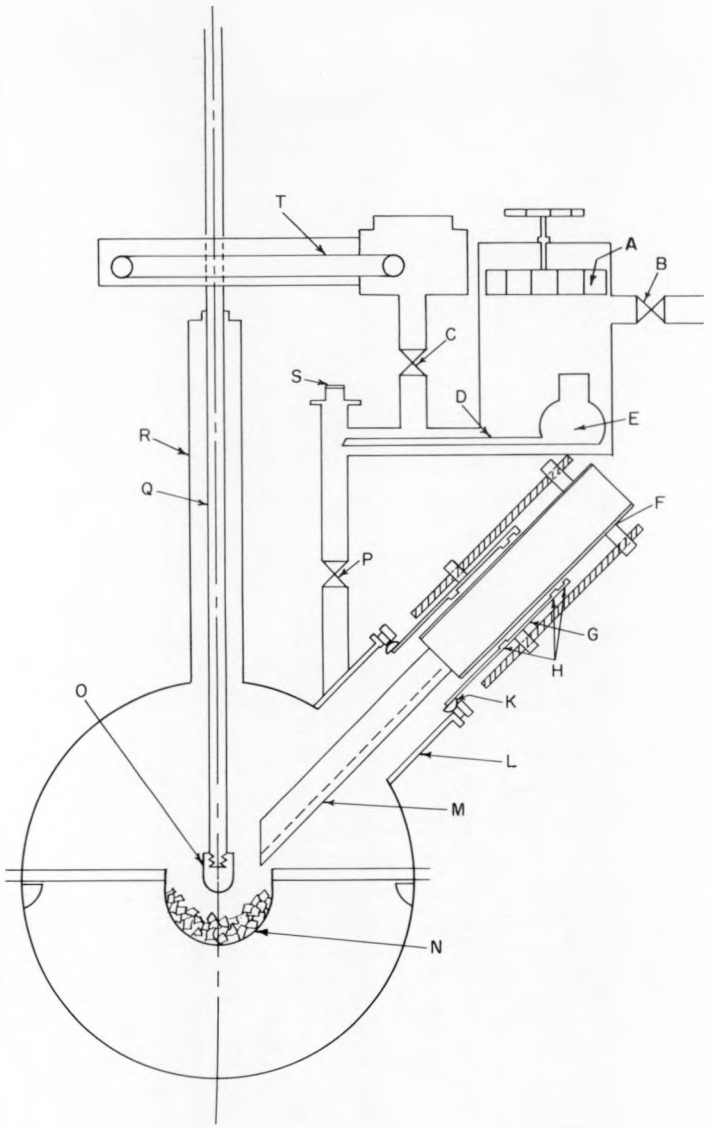

A Charge control, 14 individual charges
B Vacuum valve to pump
C Vacuum hopper valve for isolation of T from system
D Vibrator feeding from A
E Syntron vibrator
F Adjustable feed trough
G Fixed tube with balljoint
H O-ring seals
K Vacuum tight balljoint to permit positioning of M
L Fixed tube welded to chamber
M H_2O-cooled feeding trough for introducing charge into N
N Charge in crucible
O Electrode tip
P Vacuum hopper valve to isolate superstructure from furnace chamber
Q Electrode stinger
R Electrode tower
S Sight glass for observation of feed rate
T Belt for incremental charging of bulk materials

AEA 39238

FIGURE 1. SCHEMATIC DIAGRAM OF SKULL FURNACE SHOWING MODIFICATIONS FOR ALLOYING BY INCREMENTAL FEEDING TECHNIQUES

Evaluation of Various Graphites

During previous melting studies in vacuum and in an inert atmosphere, it was noted that both metallic and nonmetallic impurities in the charges appeared to produce turbulence in the melt. Spatterings from the melt eroded the graphite electrode and thereby altered the composition of the castings. For this reason, various grades of graphite were evaluated both as charge additions and as electrode tips. These graphites were evaluated on the basis of the amount of tip erosion and on the basis of the turbulence exhibited by the molten pool. AGOT, TSF, and commercial electrode grades of graphite were of particular interest because of their high density and their availability in large quantities.

Since it was found that the performance of all grades was improved by outgassing the graphites in vacuum at 760 C for 4 hr, all graphitic materials were subjected to this treatment prior to use. Using outgassed TSF graphite as both the charge addition and the electrode tip, seven successive melts were made in a single skull. The 5 to 8-kg charges contained 4.2 w/o carbon in all cases. Carbon analyses of the castings produced during this series of melts are shown in Table 1. Melting time from power-on to power-off was 25 ± 5 min.

TABLE 1. ANALYSES OF A SERIES OF SKULL-CAST INGOTS MADE USING TSF GRAPHITE

Casting	Casting Weight, kg	Carbon Content, w/o	Graphite Electrode Tip Loss, g
1	6.56	5.61	15
2	6.0	5.58	30
3	3.14	5.36	10
4	9.0	5.31	15
5	6.41	5.28	30
6	6.0	5.06	15
7	9.0	4.58	15

An examination of the seven separate TSF graphite electrode tips used in making these ingots revealed that tip erosion was minor. Tip losses ranged from a minimum of of 10 g to a maximum of 30 g. Losses of this magnitude could account for a carbon variation in the ingots of about 0.17 w/o. Therefore, it was concluded that the major portion of the carbon in the castings in excess of the 4.2 w/o in the charge was derived from the skull. Each successive melt reduced the carbon content of the skull which in turn reduced the carbon available for the following melt.

Similar series of melts were made using AGOT and commercial graphites. The chemical analyses of the castings obtained from the series of melts utilizing outgassed AGOT graphite are shown in Table 2. These results show no discernible trend other than a spread of plus 0.48 minus 0.29 w/o carbon from the intended 5.0 w/o carbon. These variations in carbon content from melt to melt are comparable to those obtained when vacuum-outgassed commercial graphite was employed to melt a charge containing 4.2 w/o carbon (Table 3). Turbulence within the melt and splashing of the melt during

TABLE 2. ANALYSES OF SERIES OF SKULL-CAST INGOTS MADE USING AGOT GRAPHITE

Casting	Carbon Content, w/o	Graphite Electrode-Tip Loss, g
1	4.8	100
2	5.48	200
3	5.33	135
4	4.95	50
5	5.37	80
6	5.24	95
7	4.71	100

TABLE 3. ANALYSES OF SERIES OF SKULL-CAST INGOTS MADE USING COMMERCIAL ELECTRODE GRAPHITE

Casting	Carbon Content, w/o	Graphite Electrode-Tip Loss, g
1	4.17	20
2	4.29	20
3	4.66	60
4	4.52	20
5	4.61	50
6	4.65	40
7	4.59	30

the solution of the outgassed graphite were not excessive, although tip erosion was both excessive and erratic. In some cases, AGOT graphite tip weight losses of up to 40 per cent were noted during melting. These large and erratic tip losses are believed to have resulted in the variable carbon contents of the castings listed in Table 2. The commercial graphite electrode tips were observed to erode at a lower rate than AGOT graphite tips. As shown in Table 3 the commercial graphite tips contributed less carbon to the melts than the AGOT graphite.

Examination of the graphite electrodes used in the above series of melts showed that the erosion rates of the TSF graphite electrodes were considerably less than those exhibited by either the commercial graphite or by the AGOT graphite. It is believed that the high density, low impurity level, and fine structure of TSF graphite are responsible for its stability in this application. The results indicate that compositional control is enhanced by outgassing the carbon addition to the melt and by using outgassed TSF graphite electrode tips. The series of melts prepared using TSF graphite tips also showed the necessity of using a homogeneous skull to obtain castings of predictable carbon content.

Evaluation of Commercial Prealloyed Uranium Carbide

The melting studies discussed in the preceding section of this report indicated two reasons for the unpredictable carbon contents exhibited by the castings: (1) erratic and unpredictable tip erosion and (2) segregation within the skull. The effects of both of these factors could be alleviated by the use of prealloyed material which could reduce or eliminate the tendency for gravity segregation and greatly reduce the melting time. Therefore, a commercially available prealloyed uranium monocarbide was obtained for study as a charge material for skull melting.

The prealloyed material used was purchased from Vitro Corporation in the form of shot of random sizes. Melting was accomplished under a dynamic vacuum in the skull-type arc-melting facility utilizing a 10-kg crucible. The charge melted quitely at 3600 amp and 22 v in less than 15 min. The fused material, essentially the complete charge, was permitted to solidify, and was removed from the skull and evaluated by chemical analysis and metallographic examination. This melt of prealloyed material was noteworthy for rapid melting, low power input and lack of gas evolution. These characteristics should reduce melting costs and aid in the control of carbon content. The lack of gas evolution visibly reduced spatter from the molten pool and, thereby, reduced tip erosion. A reduced power input and the short melting time also contributed to reduced tip erosion.

Segregation in the Skull

Stratification of uranium-rich and carbon-rich layers resulted when skulls were produced from elemental uranium and carbon in a 30-kg crucible. When such raw materials were employed, the low-melting point, high-density uranium metal melted first and tended to flow to the bottom of the charge without reacting fully with the graphite in the charge. This process resulted in a skull composed of low-carbon uranium-rich layers near the outside and bottom and a high-carbon layer in the top-center of the skull

cavity. Melting in such a nonhomogeneous skull with an arc which wanders from place to place invariably produced castings of unpredictable composition.

Since it was believed that stratification in the skull could be greatly reduced if the bulk of the material were molten throughout the melting cycle, the effect of melting both elemental and prealloyed charge materials in a small skull was studied. The use of a 10-kg crucible permitted the establishment of a molten pool which extended to the bottom of the crucible and thereby lessened the tendencies for vertical segregation. However, when elemental charges were employed even in this small crucible sufficient segregation was noted in the skulls to preclude attainment of castings of predictable composition.

Using prealloyed uranium carbide it was possible to produce a skull of uniform composition. Essentially complete homogeneity of the skull resulted from the use of prealloyed materials of uniform densities and melting points in the charge. A decrease in melting time resulted from elimination of the need to dissolve lumps of graphite. The degree of homogeneity in the skull was readily determined by visual examination.

Effects of Atmosphere on Compositional Control

Early investigations showed that the atmosphere in the furnace affects the integrity of the cast product; however, the effect of atmosphere on the composition of the castings was not determined.[3] Therefore, melts were prepared for this purpose utilizing outgassed commercial graphite for charge material and TSF graphite for electrode tips. The atmospheres of interest were a dynamic vacuum, an atmosphere of helium at 1/3 atm absolute, and a mixture of 3 parts helium and 1 part argon at 1/3 atm absolute. In all cases prealloyed charges of known composition were used in conjunction with an adequate quantity of metallic uranium to adjust the final composition to approximately 5.0 w/o carbon and to compensate for subsequent carbon pickup due to tip erosion. The quantity of elemental uranium needed for this purpose was 280 to 300 g per kg of prealloyed material. As indicated earlier, this procedure effectively eliminated segregation within the skull and resulted in castings of more uniform and predictable composition. The chemical analyses of 1-kg ingots produced under each of the above atmospheres are shown in Table 4.

A comparison of the effects of the atmospheres employed showed the following:

(1) A helium atmosphere resulted in the smallest molten pool, the most erratic arc, and the smallest castings.

(2) The least tip erosion and the most stable arc were observed when melting under a mixture of helium and argon.

(3) A dynamic vacuum resulted in the greatest tip erosion, the largest molten pool, and the soundest castings.

TABLE 4. ANALYSES OF SKULL-CAST NOMINAL URANIUM-5.0 w/o CARBON MADE TO STUDY EFFECT OF MELTING ATMOSPHERE ON CASTING COMPOSITION

Furnace Atmosphere	Ingot	Specimen Location	Carbon Content, w/o
Dynamic Vacuum	7	Top	5.16
		Bottom	5.19
	8	Top	5.22
		Bottom	5.21
	9	Top	5.13
		Bottom	5.16
1/3 atm of He	10	Top	5.19
		Bottom	5.18
	11	Top	5.09
		Bottom	5.14
	12	Top	5.40
		Bottom	5.12
1/3 atm 25 A-75 He	13	Top	4.95
		Bottom	4.95
	14	Top	4.96
		Bottom	4.91
	15	Top	4.97
		Bottom	4.91

If proper attention is given to establishing a homogeneous skull as by using prealloyed material as the bulk of the material in the charge, good reproducibility of composition can be attained regardless of the atmosphere employed. The chemical analyses in Table 4 show that under a given atmosphere variations in carbon content generally less than 0.05 w/o can be expected in replicate melts. The higher carbon content exhibited by the vacuum-melted materials is a result of the greater tip erosion experienced when melting in this atmosphere and can be compensated for by increasing the quantity of elemental uranium used in the charge. In terms of economy, an atmosphere consisting of a dynamic vacuum is the most advantageous, since it yields a greater quantity of molten material and results in a superior casting. If casting integrity is less critical, then the use of an atmosphere of a mixture of helium and argon can be recommended.

Compositional Control During Melting

The studies discussed in the preceding sections showed that the composition of uranium-carbon castings could be controlled within very narrow limits when prealloyed material was used to prepare the skull and the majority of the charge. The cost of producing castings entirely from prealloyed stock is inherently greater than the cost of production of castings from elemental materials, assuming that the total cost of buying or preparing prealloyed melting stock is greater than the cost of elemental

materials. Also the procedure provided no method of compensating for graphite additions to the melt from unexpected or unusual erosion of the graphite tip. Since significant cost reductions could be realized through the use of elemental charge materials and because it was believed that quantitative rather than empirical control of carbon content could be attained, a hopper and feed mechanism was installed on the skull-melting furnace. A description of this mechanism can be found in the section on equipment.

Twelve melts were prepared under a dynamic vacuum using TSF graphite electrodes in the modified furnace to evaluate the preparation of charges and skulls directly from elemental materials. The first melt in the series was intended to prepare a complete skull from virgin melting stock. A charge of 4 kg of unalloyed material containing 4.2 w/o carbon was charged in the skull in four increments and melted. A power input of 3700 amp and 22 v was used. An extremely small molten pool was obtained, and severe segregation was noted visually. This segregation was identical in all major respects to that noted in previous melts employing elemental charges.

The second melt in the series utilized an initial charge of 4 kg of prealloyed uranium-5.0 w/o carbon alloy. This charge was melted using the above-mentioned power level. When the molten pool attained a size approximating one-half the diameter of the crucible, elemental mixtures of uranium plus 4.5 w/o carbon were slowly added to the melt. This power input proved insufficient to dissolve the elemental additions completely in a reasonable length of time. The casting from this melt contained 4.5 w/o carbon, and the residual skull proved to be inhomogeneous. The next six melts were made in a similar manner using a charge composition of 4.8 w/o carbon and altering the rate of additions and power level with each melt. In every case some unmelted graphite was noted in the skull after pouring the casting, and the carbon content of the castings was less than that desired.

Four final melts were made using a power input of 4300 amp and 28 v. The skull was prepared utilizing 4 kg of prealloyed uranium-5.0 w/o carbon as the initial charge. Additions to the molten charge were begun when the molten pool covered approximately seven-eights of the crucible area, and the rate of additions was such that it increased as the size of the molten pool increased. The utilization of incremental feeding reduced the tendency for gravity segregation in the melt, since any increment introduced into the melt was consumed before further additions are made.

Observations during melting and examination of the skull after melting revealed that the increased power level increased the depth of the molten pool to approximately twice that attained at 3700 amp and 22 v. Complete solution of all material added to the melt was achieved. Castings 2 in. in diameter by 6 in. long with excellent surfaces were produced from elemental additions of 5.5 to 6.0 kg. These castings were evaluated by metallographic examination and radiographic techniques. The evaluation revealed good compositional control from casting to casting and from end to end within a casting as shown in Table 5.

TABLE 5. ANALYSES OF A SERIES OF 6-KG SKULL-CAST INGOTS NOMINALLY CONTAINING 5.0 w/o CARBON PRODUCED UTILIZING INCREMENTAL FEEDING TECHNIQUES

Ingot	Specimen Location	Analytical Technique	Carbon Content, w/o
9	Top	Metallographic	4.95
	Bottom	Metallographic	5.00
10	Top	Chemical	5.04
	Bottom	Metallographic	5.00
11	Top	Chemical	4.99
	Bottom	Metallographic	4.95
12	Top	Chemical	4.99
	Bottom	Metallographic	4.95

The above series of melts showed that high-quality castings could be produced from elemental melting stock within essentially the same compositional limits attained with prealloyed melting stock provided that the skull is made up initially from prealloyed material. The charge mechanism permitted the formation of a homogeneous melt from elemental materials in a single melting operation.

The potential ability of the charging mechanism to produce a complete series of castings without the delays associated with opening the furnace and exposing the skull to the atmosphere was not investigated. With the addition of the proper indexing and molding equipment it should be possible to make up to eight skull castings in the current furnace without opening the vacuum chamber. This would result in great savings by eliminating much of the time ordinarily required for charging and evacuating the furnace.

Conclusions

The melting procedures and equipment described are capable of producing castings of reproducible carbon content by either of two techniques: (1) the use of prealloyed charges supplemented with minor additions of uranium and (2) the use of elemental charges introduced slowly into the molten pool during melting. The former technique is probably more costly, since it requires either the use of prealloyed melting stock or two melting operations with an intermediate carbon analysis.

The composition of castings can be controlled within very narrow limits under any one of three atmospheres by melting prealloyed charges supplemented with metallic uranium. Replicate melts prepared in a dynamic vacuum varied from one another in composition by less than ±0.05 w/o carbon; melts prepared under partial pressure of helium varied from one another by less than ±0.2 w/o carbon; melts prepared under a partial pressure of helium and argon varied from one another by less than ±0.05 w/o carbon. Variations from the intended composition were somewhat greater. This degree of control can only be attained when the initial skull is homogeneous and of known composition. Where the initial skull is inhomogeneous, the carbon content of replicate melts is unpredictable. Of the three grades of graphites tested, TSF graphite was the

least susceptible to erosion during melting. Melting under a dynamic vacuum resulted in the largest molten pool in the skull at a given power level, and casting under these conditions resulted in the soundest castings.

Homogeneous melts can be prepared from elemental materials by charging raw materials in small increments to a skull prepared from prealloyed uranium carbide. The composition of castings made by this incremental charging technique can be predicted and controlled to within ±0.05 w/o carbon. It is possible that the equipment can be further modified to produce additional castings without opening the furnace and exposing the skull to possible contamination from the atmosphere. The technique may be further developed to permit the operator to adjust the melt composition during melting to compensate for any unexpected tip erosion.

MECHANICAL AND PHYSICAL PROPERTIES OF URANIUM-CARBON ALLOYS

The measurement of mechanical and physical properties of uranium-carbon alloys was the prime concern of the portion of the program discussed in this section. Of particular interest were strength, hardness, thermal expansion, electrical resistivity, and thermal conductivity measured at room and elevated temperatures. Also of interest were the effects of alloy additions and heat treatment on the properties of uranium carbide.

During the previous portions of this program corrosion tests of uranium-carbon alloys containing 4.5 to 9.5 w/o carbon were conducted in water at 60 C, ethylene glycol at 150 C, and Santowax R at 350 C.[3] The results showed a trend toward lower corrosion rates near 7.0 w/o carbon and toward higher corrosion rates near UC (4.8 w/o carbon) and UC_2 (9.2 w/o carbon). It was found that water attacks uranium carbides of all compositions extremely rapidly even at temperatures as low as 60 C. Considerable mechanical-property data also were obtained. Compressive rupture strengths of 51,100 psi for a 4.8 w/o carbon alloy and 65,700 psi for a 7.0 w/o carbon alloy were reported.[3] Measurements of hardness and electrical resistivity at room temperature were reported.

The phase of the program discussed in this report (Phase III) dealt mainly with obtaining measurement of hardness, thermal expansion, thermal conductivity, and electrical resistivity at temperatures above 1000 C. Changes in microstructure associated with high-temperature heat treatments were studied also and were used to clarify some areas of the uranium-carbon constitution diagram.

Hot Hardness

The hot hardness of uranium-carbon alloys containing 5.0, 7.0, and 9.0 w/o carbon was measured in the 1000 to 1500 C temperature range. The results of these measurements are presented in Table 6, and plots of the logarithm of hardness versus temperature for the 5.0, 7.0, and 9.0 w/o carbon alloys are shown in Figure 2.

TABLE 6. HOT HARDNESS OF URANIUM-CARBON ALLOYS

Temperature, C	Hardness of Alloys[a], DPH					
	5 w/o Carbon		7 w/o Carbon		9 w/o Carbon	
	Specimen 1	Specimen 2	Specimen 1	Specimen 2	Specimen 1	Specimen 2
1000	780	374	(b)	(b)	679	185
1100	270	95	318	115	464	105
1200	130	30	49	43	340	66
1300	70	16	17	38	274	51
1400	40	12	8	11	203	40
1500	22	10	2	7	163	21

(a) Hardness numbers reported are averages of five measurements at each temperature.
(b) Indentations too small for accurate measurements.

Tests were conducted in a vacuum using a zirconia indenter rod and a 1-kg load. Each hardness value given in Table 6 represents the average of measurements of five indentations. The data demonstrated considerable scatter. Scatter of readings was caused, to some extent, by severe irregularity of the indenter impressions. Such irregularities occurred as a result of erosion of the pyramid-shaped indenter tip during testing. Although the hardness measurements were not conclusive, they indicated that UC, U_2C_3, and UC_2 all soften at relatively high temperatures. Plotting the logarithm of the hardness with temperature gave a relatively straight line above 1000 C. By including the room-temperature hardness (determined with a diamond indenter) in the plot, a change in slope indicates a softening point.

Microstructural Analysis of Uranium-Carbon Alloys

The microstructures of three uranium-carbon alloys in the 5.9 to 6.5 w/o carbon range were studied metallographically. The structure of as-cast uranium-5.9 w/o carbon alloy consisted of UC and UC_2 needles, the latter of which were heavily concentrated at grain boundaries (Figure 3a). Inspection of a 6.2 w/o carbon alloy revealed an intimate two-phase mixture of UC and UC_2 (Figure 3b) considered indicative of a eutectic. The microstructure of a 6.5 w/o carbon alloy consisted of UC_2 and UC needles with UC predominantly present at grain boundaries (Figure 3c). These structures indicate a minimum in the liquidus curve at a composition of about 6.2 w/o carbon. This minimum may be associated with a eutectic, or it may be simply a minimum in the liquidus. To help identify the region below the minimum, a specimen of the 6.5 w/o carbon alloy was held for 20 min at a temperature of 2050 C. Subsequent inspection of the structure indicated that the alloy had been heated in a two-phase region (Figure 4a). The metallographic appearance of specimens of the 6.5 w/o carbon alloy heated first for 5 min at 2100 C and then for 2 min at 2300 C (Figure 4b) was interpreted to indicate that the alloy had entered a single-phase region. This also appeared to be the case when a specimen of the 6.2 w/o carbon alloy was held 5 min at 2200 C. The uranium-carbon constitutional diagram shown in Figure 5 incorporates these findings.

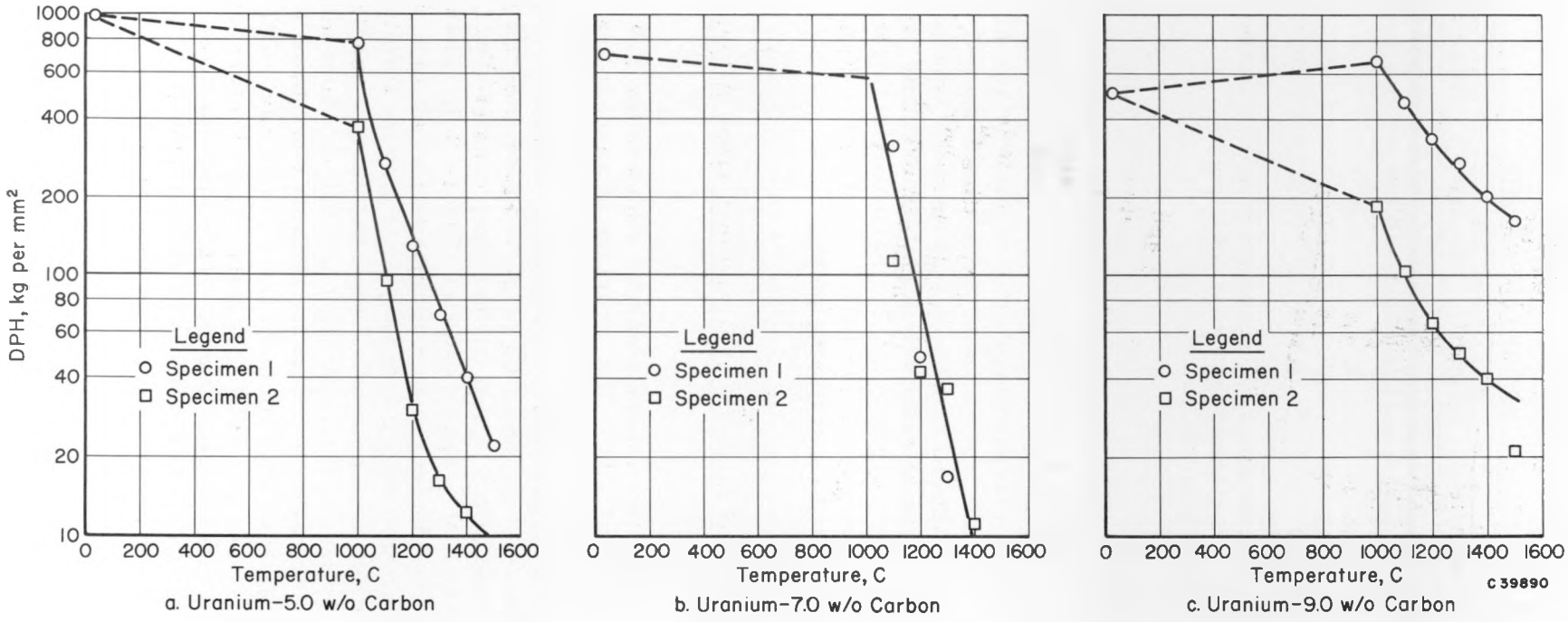

FIGURE 2. HOT-HARDNESS VALUES FOR URANIUM CARBIDE

250X RM17984

a. Uranium-5.9 w/o Carbon

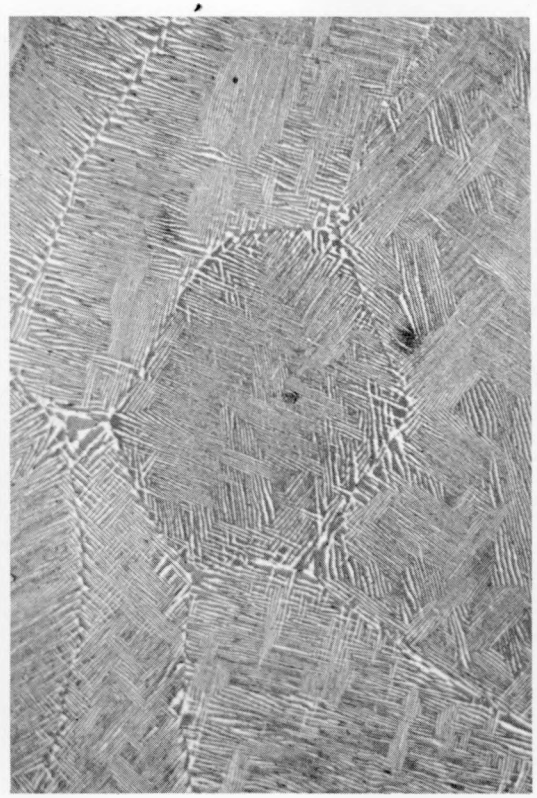

250X RM17982

b. Uranium-6.2 w/o Carbon

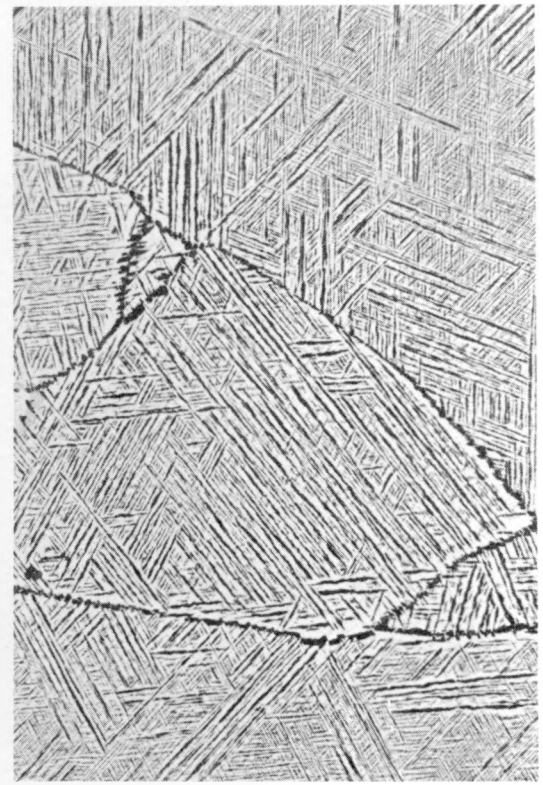

250X RM17983

c. Uranium-6.5 w/o Carbon

FIGURE 3. TYPICAL MICROSTRUCTURES OF CAST URANIUM-CARBON ALLOYS

A mixture of UC_2 (white) and UC (gray) is evident in each photomicrograph.

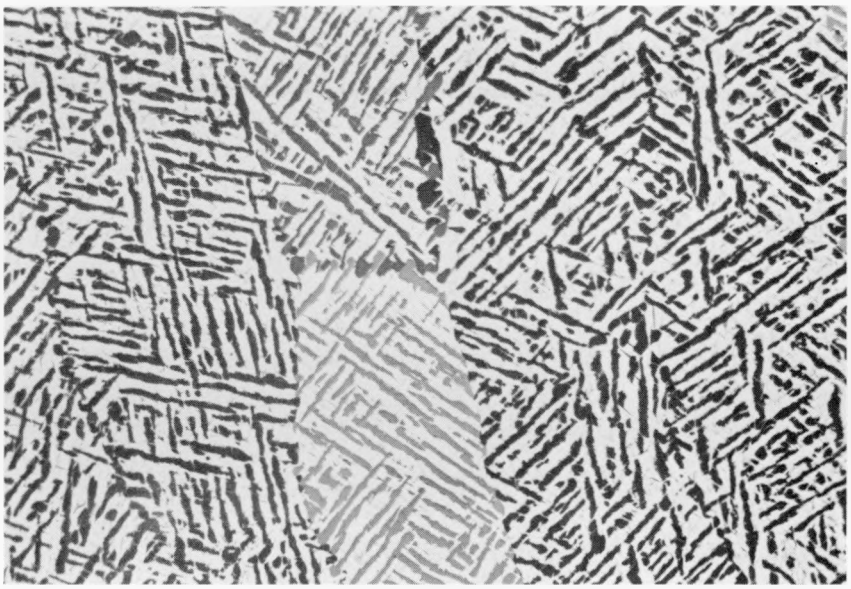

250X RM17848

a. Heated 20 Min at 2050 C

The alloy appears to have been heated in a two-phase region.

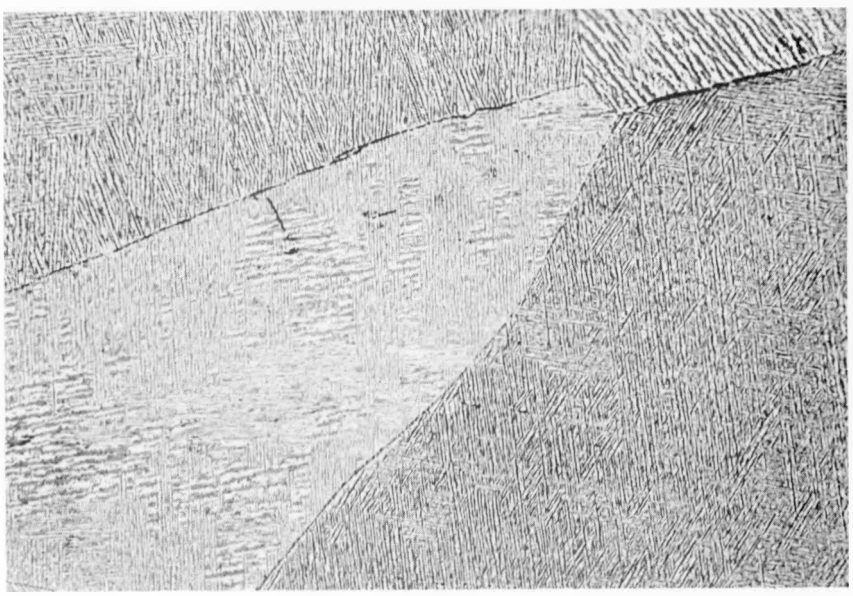

100X RM17883

b. Heated 5 Min at 2100 C and then 2 Min at 2300 C

The alloy appears to have entered a single-phase region.

FIGURE 4. EFFECT OF HEAT TREATMENT ON URANIUM-6.5 w/o CARBON TO SHOW A REGION OF SOLID SOLUBILITY BETWEEN UC AND UC_2 AT HIGH TEMPERATURE

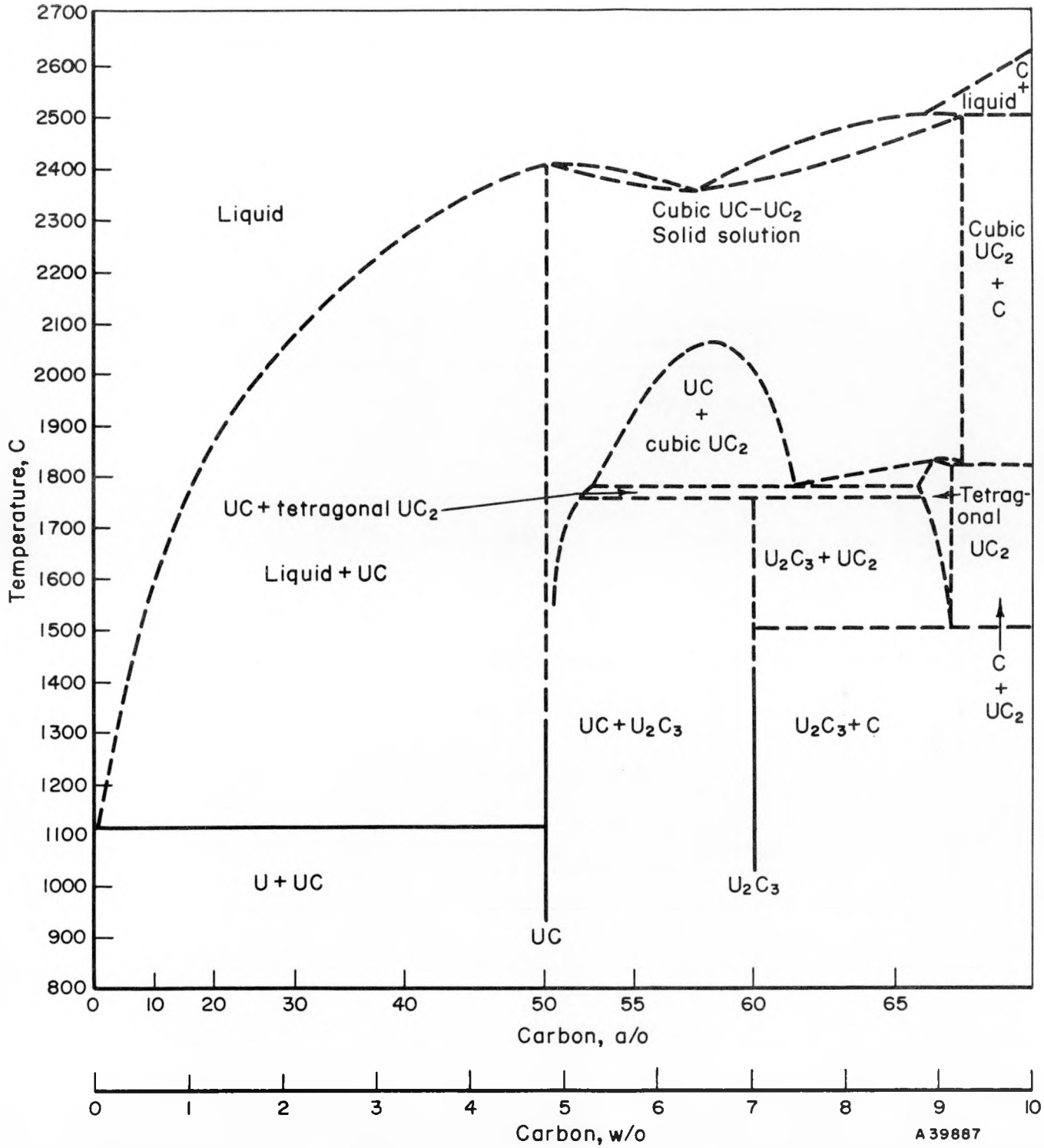

FIGURE 5. URANIUM-CARBON CONSTITUTIONAL DIAGRAM

Transformation Characteristics of Uranium Sesquicarbide

Preliminary measurements of the transformation characteristics of uranium-7.0 w/o carbon alloys into uranium sesquicarbide were attempted. For this purpose, as-cast samples of uranium-7.0 w/o carbon alloys, showing a typical intimate mixture of UC and UC_2 by metallography (Figure 6a), were reheated to various temperatures for various lengths of time. On cooling, the samples were re-examined metallographically and those samples which showed a single-phase equiaxed structure were assumed to be fully transformed to U_2C_3 (Figure 6b). Those samples which showed the original structure or a fuzzy-feathery structure were assumed to be incompletely transformed to U_2C_3. The results of these studies are shown in Table 7. These data suggest that the nucleation and growth process for crystallites of U_2C_3 is sluggish.

TABLE 7. PRELIMINARY MEASUREMENTS OF THE RATE OF TRANSFORMATION OF URANIUM-7 w/o CARBON ALLOYS FROM THE AS-CAST CONDITION (UC PLUS UC_2) TO URANIUM SESQUICARBIDE (U_2C_3)

Temperature, C	Estimated Time for Complete Transformation, hr
1700	Less than 1/4
1600	Less than 1/4
1500	1/4
1400	1
1200	More than 100
1100	More than 1000

Thermal Expansion

The thermal-expansion properties of arc-cast uranium-carbon alloys containing 4.8, 7.0, and 9.0 w/o carbon were determined, and the results are presented in Figures 7, 8, and 9 for each alloy, respectively. The thermal-expansion characteristics of the 4.8 and 7.0 w/o carbon alloys were similar; the rate of expansion of the 9.0 w/o carbon alloy was substantially higher in each temperature range investigated.

Electrical Resistivity

Electrical-resistivity measurements were obtained on alloys of compositions similar to those used in the thermal-expansion measurements. Temperatures ranged from room temperature to 1600 C. Resistivities of the 4.8, 7.0, and 9.0 w/o carbon alloys are plotted versus temperature in Figure 10. From the data, it is apparent that the electrical resistivity of the uranium-carbon alloys increases with increasing carbon content. The resistivity of the 7.0 w/o carbon alloy is only slightly higher than that of the 4.8 w/o carbon alloy at corresponding temperatures. On the other hand, the

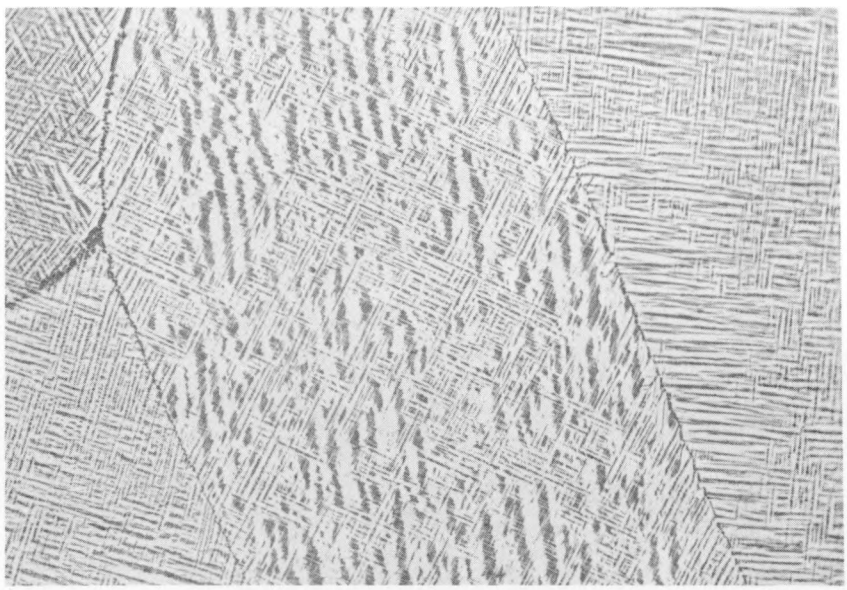

250X RM16814

a. As-Cast Alloy

A fine eutectoid mixture of black UC and white UC_2 is visible.

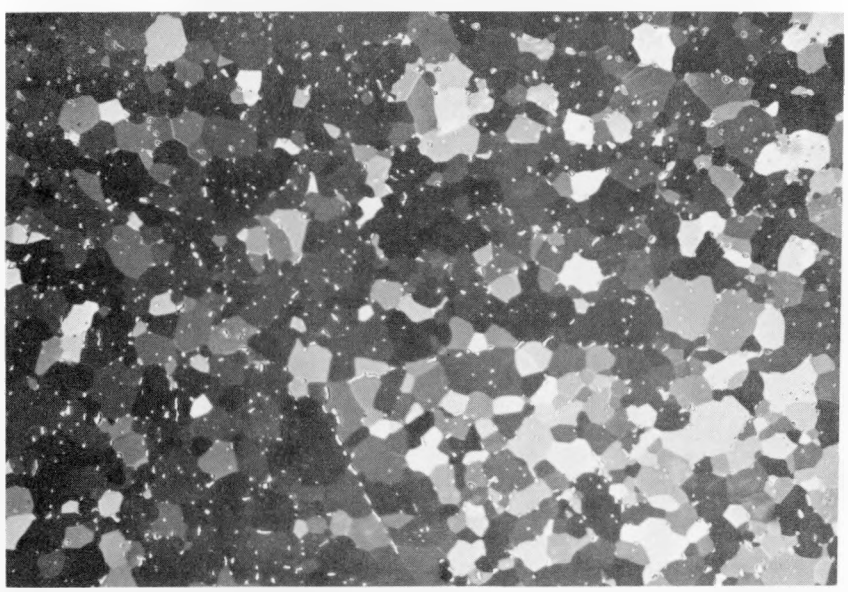

250X RM16799

b. Heated 15 Hr at 1400 C

Equiaxed U_2C_3 structure is evident. Some residual UC or UC_2 is present as white flecks.

FIGURE 6. TRANSFORMATION OF URANIUM-7.0 w/o CARBON ALLOY TO U_2C_3 DURING HEAT TREATMENT

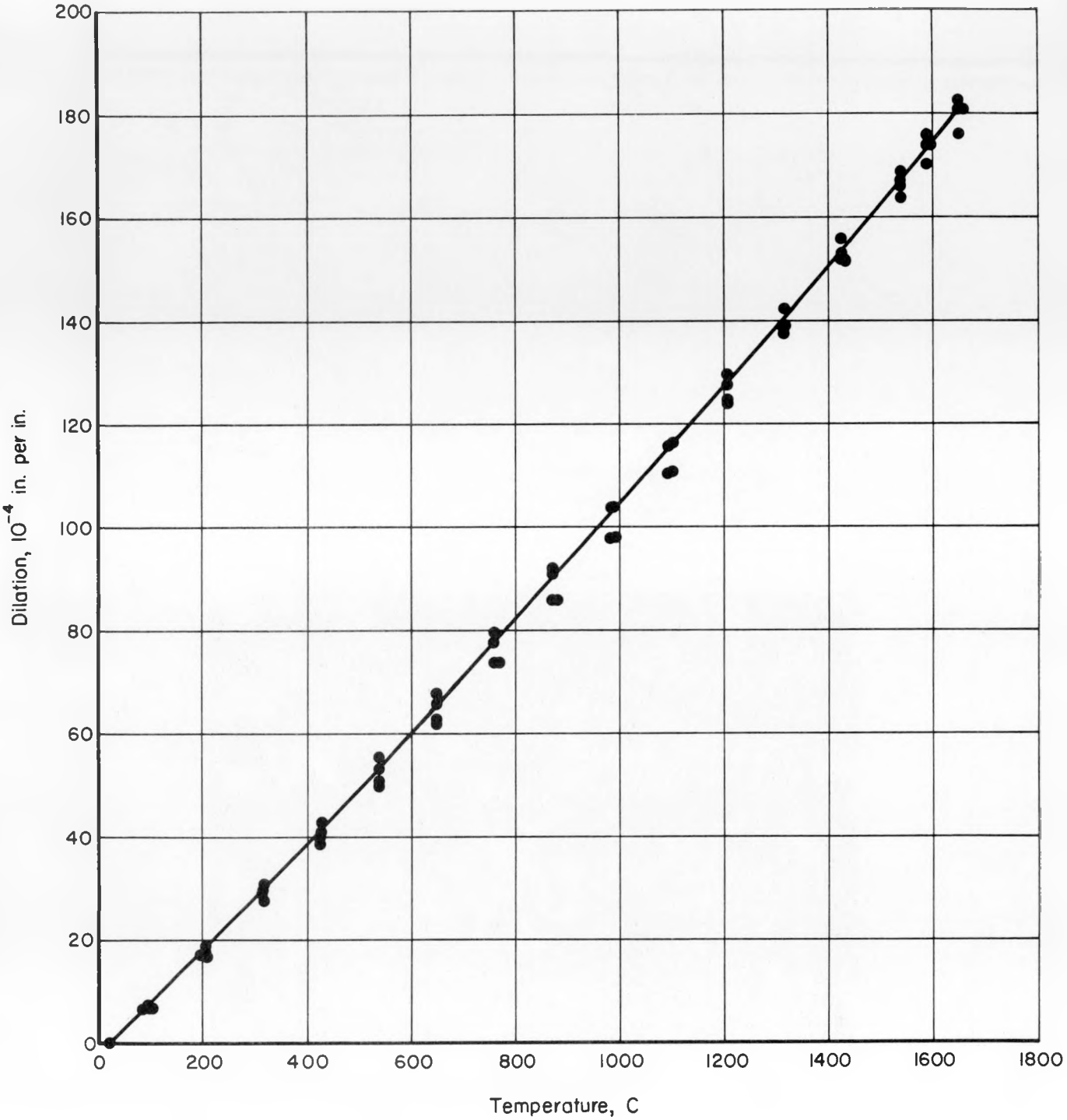

FIGURE 7. DILATION OF AS-CAST URANIUM-4.8 w/o CARBON ALLOY

Heating rate: 4 C per min.

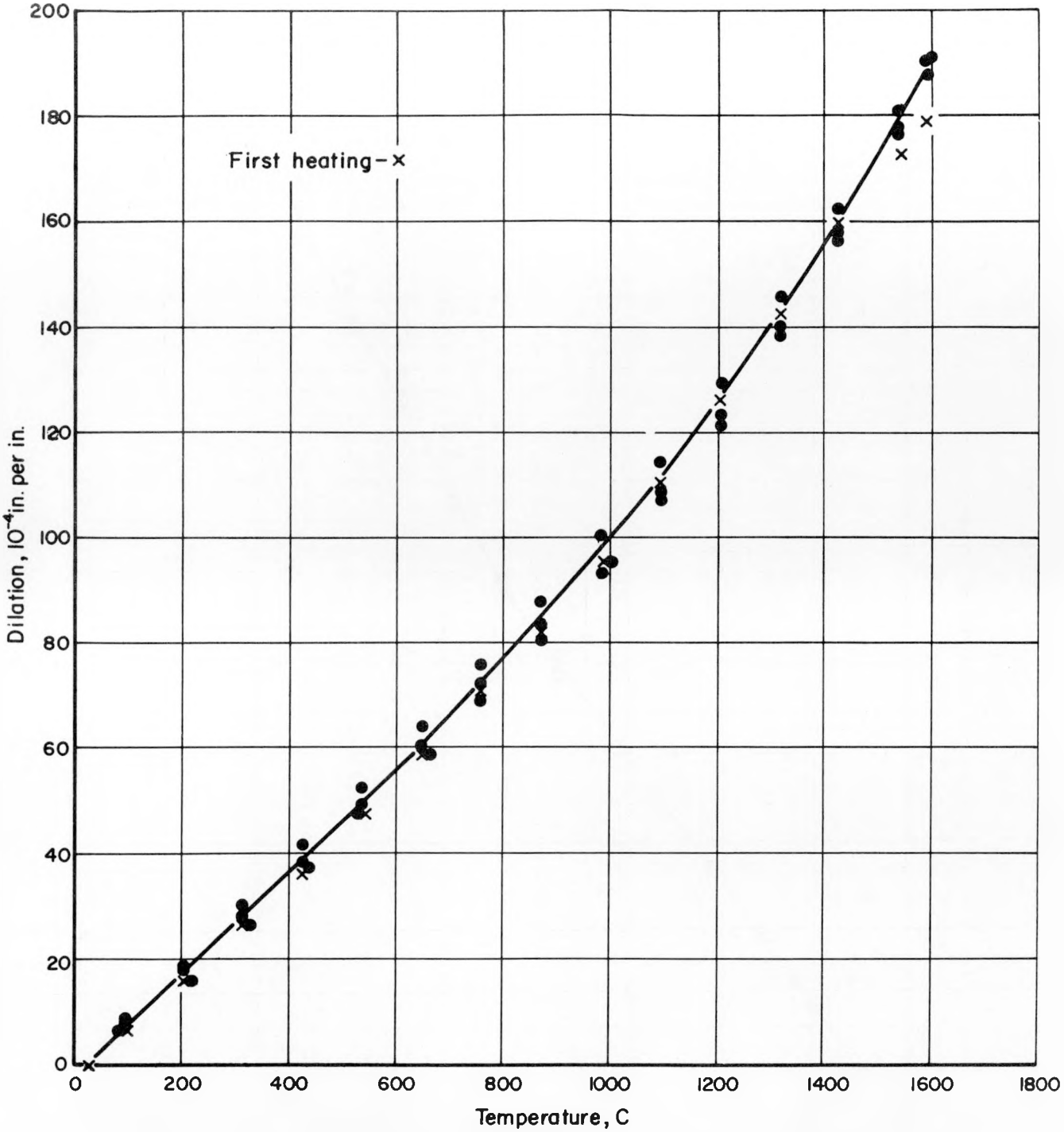

FIGURE 8. DILATION OF AS-CAST URANIUM-7.0 w/o CARBON ALLOY

Heating rate: 4 C per min.

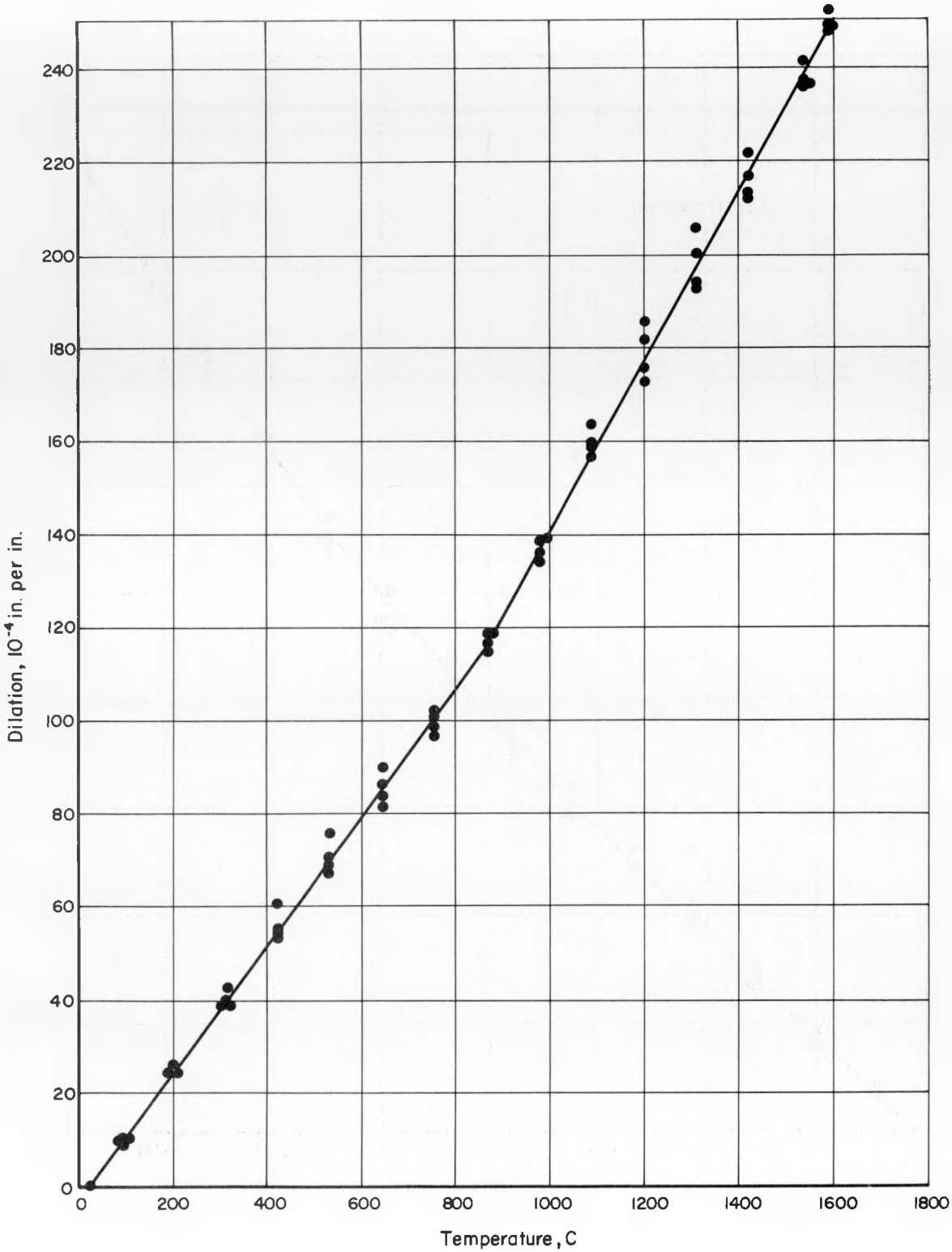

FIGURE 9. DILATION OF AS-CAST URANIUM-9.0 w/o CARBON ALLOY

Heating rate: 4 C per min.

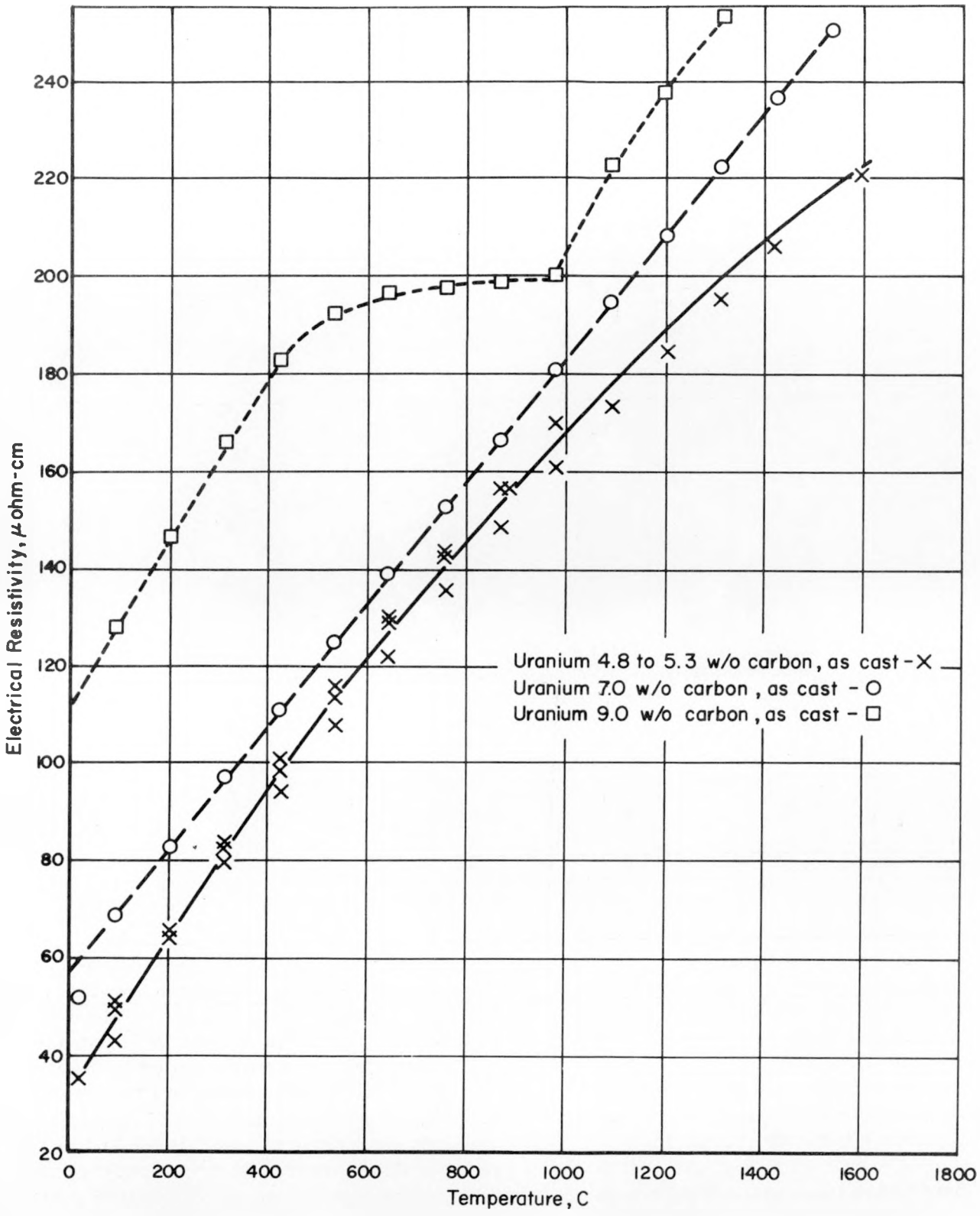

FIGURE 10. EFFECT OF TEMPERATURE ON THE ELECTRICAL RESISTIVITY OF URANIUM-CARBON ALLOYS

resistivity of the 9.0 w/o carbon alloy is roughly twice that of the 4.8 w/o carbon alloy (UC) at temperatures up to 600 C. A change in shape in the resistivity and dilation plots at about 870 C for the uranium-9.0 w/o carbon alloy suggests a change in state.

The specimens used in both the electrical-resistivity and the thermal-expansion measurements were examined after testing and found to be sound. Although these tests were conducted in vacuum, the specimens were contaminated at the surfaces (Figure 11). Since this surface effect on the specimens was slight, it was believed that it had little, if any, influence on the results of the property measurements.

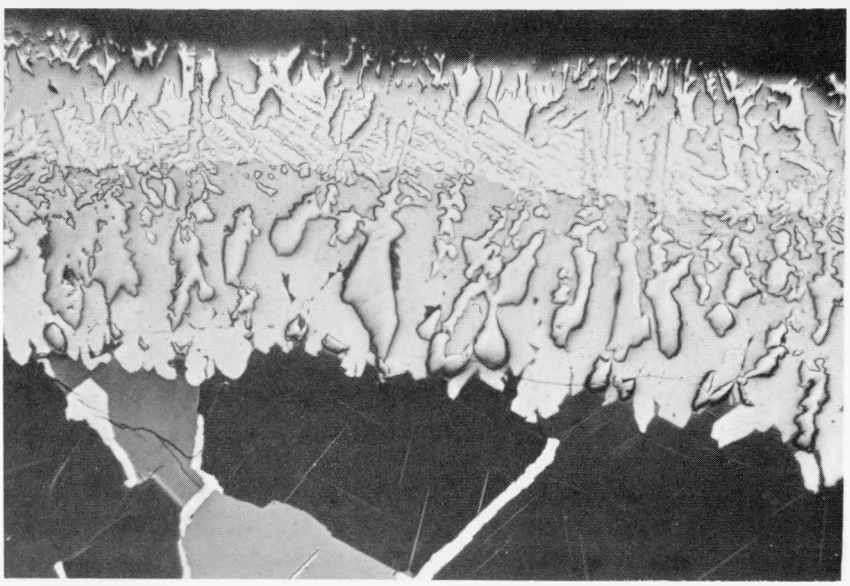

250X RM19174

FIGURE 11. EXAMPLE OF CONTAMINATED SURFACE EXHIBITED BY ELECTRICAL-RESISTIVITY AND THERMAL-CONDUCTIVITY SPECIMENS AFTER TESTING

Thermal Conductivity

An attempt was made to determine the thermal conductivity of a uranium-5.0 w/o carbon alloy at high temperatures. The specimen consisted of two semicircular disks, 3.3 in. in diameter by 0.94 in. in thickness. These pieces were wired together to form a single circular disk. The composite disk was placed on a Type 347 stainless steel heat-flow meter. The meter, which was calibrated, was surrounded by several protection rings, and the entire assembly was attached (by silver solder) to a water-cooled copper heat sink. A carbon heat manifold was positioned on top of the specimen and directly beneath carbon heaters. Carbon cloth separated the specimen at the top from the manifold and at the bottom from the heat-flow meter. Thermocouples, used to determine temperature differentials radially in the specimen, were located just below the two surfaces and at the center of the specimen. Thermocouples were comprised of platinum and platinum-10 w/o palladium alloys.

The thermal conductivity of one part of the specimen was found to be 0.2 w/(cm)(C). Little variance from this value was noted at any temperature up to 1140 C, the point at which measurements on this part of the specimen ceased because of failure. The other side of the specimen measured 0.12 w/(cm)(C) up to a temperature of 1500 C. Although both portions of the specimens were fabricated from the same casting and were of the same composition, the portion having the lower conductivity was found to contain some cracks after testing. There was also a nitride film on the specimen, probably caused by nitrogen in the argon which was used in the testing chamber.

DIFFUSION STUDIES OF URANIUM MONOCARBIDE

The complete details of a series of diffusion studies of uranium monocarbide performed in this program are contained in a separate report (BMI-1551).[1] The diffusion coefficients obtained for self-diffusion of carbon and uranium in uranium monocarbide are shown in Table 8. These data for the self-diffusion of carbon in uranium monocarbide between 1200 and 1940 C fit the equation, $D_C = 0.020 \exp(-50,000/RT)$. These data for the self-diffusion of uranium in uranium monocarbide between 1600 and 2120 C fit the equation, $D_u = 0.0013 \exp(-64,000/RT)$. At temperatures between 1200 and 2200 C, D_C is about 1000 times greater than D_u.

TABLE 8. SELF-DIFFUSION COEFFICIENTS OBTAINED FOR DIFFUSION OF URANIUM AND CARBON IN URANIUM MONOCARBIDE

Temperature, C	Self-Diffusion Coefficient, cm^2 per sec	
	Uranium in UC	Carbon in UC
1200	--	1.5×10^{-9}
1500	--	1.0×10^{-8}
1500	--	1.2×10^{-8}
1600	7.0×10^{-11}	3.8×10^{-8}
1700	3.8×10^{-11}	--
1800	4.2×10^{-10}	2.0×10^{-7}
1900	8.7×10^{-10}	--
1940	--	1.1×10^{-7}
2000	5.1×10^{-10}	--
2020	6.1×10^{-10}	--
2120	2.3×10^{-9}	--

The diffusion data suggest that processes and properties dependent upon diffusion of carbon in uranium monocarbide will become active at about 800 C. Decarburization of uranium carbide by metals and reaction of uranium monocarbide with uranium dicarbide to form uranium sesquicarbide are examples of some of the processes that may be expected to occur at such low temperatures.

Processes and properties dependent upon diffusion of uranium in uranium monocarbide will become active at about 1300 C. Deformation processes such as densification by hot pressing and swelling and creep from fission-gas pressure, for example, may be expected to be very limited below approximately 1300 C.

MECHANISM OF IRRADIATION DAMAGE

Earlier studies of the effects of irradiation on uranium monocarbide resulted in indications of excellent radiation stability.[4,5] The work reported here was undertaken to establish a more detailed understanding of the mechanisms causing damage during irradiation. Measurements of property changes such as electrical resistivity, lattice expansion, and elastic strain as a function of irradiation exposure and temperature were made. Similar studies were also conducted on higher-carbon-content alloys of the uranium-carbon system to supplement the other studies and to gain an understanding of the irradiation stability of alloys of the compositions of U_2C_3 and UC_2. It was anticipated that these supplemental studies might help explain some of the phenomena observed in earlier irradiation experiments.[6]

Experimental Procedures

The specimens and capsules used in these experiments were fabricated at Battelle and were irradiated in the BRR. Upon completion of the irradiations the capsules were opened and the specimens examined in the Battelle Hot-Cell Facility. Details of the specimen-fabrication techniques, capsule designs, irradiations, and postirradiation examinations are discussed below.

Preparation of Uranium Carbide

The uranium monocarbide specimens used in the irradiation studies were made by alloying metallic uranium with crushed spectrographic-grade carbon. These materials were consolidated into buttons by arc-casting techniques. Melting was done in a water-cooled copper crucible under a helium atmosphere in a charge-flipping arc furnace with a carbon-tipped electrode. Each button was flipped over and remelted seven times in order to insure homogeneity. The final cylindrical UC castings were made from these buttons by a drop-casting technique. This method involved placing a button over the opening of a graphite thimble mold and heating sufficiently with an electric arc to cause all of the UC to melt and drop into the cylindrical mold.[2] Using this technique, sound homogeneous castings of 98 to 100 per cent of theoretical density were produced. Specimens, 1/2 in. in length by 1/4 in. in diameter were machine ground from the castings with a resin-bonded diamond wheel using Withrow-803, light machine oil, as a coolant.

Irradiation of the uranium-carbon fuel materials was performed in six capsules at the Battelle Research Reactor. The first two of these capsules, BRR-1 and BRR-2, each contained six specimens of natural uranium-5.0 w/o carbon alloy. These specimens were annealed for 1 hr at 1800 C to relieve casting stresses before irradiation.

Irradiation conditions included target burnups of 0.01 and 0.03 a/o of the uranium at about 150 C.

Capsules BRR-3, BRR-4, and BRR-5 each contained six specimens representing combinations of three different uranium-carbon alloys made from 10 per cent enriched uranium. These alloys were uranium-5.0 w/o carbon, uranium-6.7 w/o carbon, and uranium-8.5 w/o carbon. The target burnup for Capsule BRR-3 was approximately 0.15 a/o of the uranium at temperatures of about 150 C. Target burnups for Capsules BRR-4 and BRR-5 were 0.1 and 0.7 a/o, respectively, of the uranium at temperatures of 540 to 870 C. The uranium-6.7 w/o carbon and uranium-8.5 w/o carbon specimens in these capsules were all heat treated prior to irradiation; whereas the uranium-5.0 w/o carbon specimens in Capsules BRR-3, BRR-4, and BRR-5 were irradiated in both the as-cast and heat-treated conditions. The heat-treated uranium-5.0 w/o carbon specimens were held 5 hr at 1450 C primarily for the purpose of relieving casting stresses. The specimens of uranium-6.7 w/o carbon were heat treated at 1400 C for 14 hr to transform the specimens to an equilibrium structure of U_2C_3 with some residual UC present. The uranium-8.5 w/o carbon specimens were also heat treated at 1400 C for 15 hr to relieve casting stresses.

Capsule BRR-6 contained 10 per cent enriched 5.0 w/o carbon specimens in both the as-cast and the heat-treated (5 hr at 1450 C) conditions. The target burnup for these specimens was 0.7 a/o of the uranium at temperatures ranging from 540 C to 870 C.

Preparation of Capsules

In order to satisfy the desired conditions of this irradiation program, two capsule designs were utilized. The design used for the three low-temperature irradiation capsules consisted of a single-walled stainless steel tube. Six fuel specimens were positioned in each capsule by a stainless steel expanded-metal basket immersed in a liquid-metal coolant, NaK. The capsules were designed to maintain specimen temperatures below 260 C during irradiation in a specified neutron flux. Temperature monitoring systems were not incorporated in these capsules. However, dosimeter wires (nickel-0.6 w/o cobalt) were placed around each specimen basket to monitor the fast and thermal flux. The capsules were also designed to permit sampling of fission gases after irradiation.

Three capsules were designed to operate at temperatures ranging from 760 to 870 C. The specimens in a sealed inner shell were centered in a NaK bath by means of a niobium tube. The niobium tube was considered necessary to limit the decarburization which would occur if the specimens should contact the inner stainless steel shell. An outer shell was separated from the inner shell by a narrow gas annulus. This gas space provided an opportunity to achieve some degree of specimen temperature control by changing the conductivity of the gas during irradiation. Two thermocouples were positioned in the NaK to monitor the surface temperatures of two specimens in each capsule during irradiation. Also, as in the low-temperature capsules, standard cobalt-bearing dosimeter wires were placed adjacent to the niobium tube to obtain flux data. Since it has been found that uranium carbide has a strong affinity for oxygen at high temperatures,[7] a special purification of the NaK was performed in which the oxygen was gettered from the liquid-metal coolant. Special precautions were also taken in cleaning and deoxidizing the capsule parts prior to assembly.

Capsule Disassembly and Fission-Gas Sampling Procedures

The sampling of fission gas contained in the capsules was performed by drilling through the one end of each capsule and collecting the gas in an evacuated transfer system. The gas collected from each capsule was transferred into two large collection vials and ultimately to smaller vials for analysis. The gas in these vials was analyzed with a gamma-ray spectrometer to determine the quantities of krypton-85 present in each capsule.

After completion of the fission-gas sampling, each capsule was opened with a pipe cutter and the NaK was reacted with butyl alcohol. After the NaK-alcohol reactions were complete, the specimen container in each capsule was removed from the capsule and each specimen identified.

Postirradiation Evaluation Procedures

The pre- and postirradiation measurements of physical dimensions were performed using standard friction-thimble micrometers having an accuracy of at least ±0.0005 in. The density of each specimen was measured before and after irradiation by standard immersion techniques in carbon tetrachloride. Electrical-resistivity measurements were obtained employing the four-probe technique in which a fixed electrical current is passed through the specimen and the voltage drop over a known length of specimen is measured. These measurements were performed at room temperature to detect gross resistivity changes. Specimens for X-ray diffraction analysis were prepared by crushing whole specimens remotely under an argon atmosphere and collecting about 25 mg of the crushed powder, sieved through a 325-mesh screen, in a plastic holder with a 1/4-mil Mylar film window. These plastic holders were mounted on a lead plug designed to fit into a lead-shielded specimen support on a General Electric X-ray diffractometer. Radiation from the specimen was prevented from affecting the X-ray detector by specimen shielding and by use of a crystal monochromator path.

Metallographic polishing and etching of representative specimens were performed using remote handling techniques. The surface of each specimen was replicated by pressing thin sheets of cellulose-acetate wet with methyl acetate on the etched specimen and drying for about 1/2 hr. The cellulose acetate replicas were then pulled from the surface of the specimens and cut to size. The replicas were then mounted on glass plates and prepared for examination under the electron microscope.

Effects of Irradiation

Evaluation of Uranium-5.0 w/o Carbon Alloy

The uranium-5.0 w/o carbon alloy specimens contained in the first two capsules were fabricated from natural uranium and were annealed for 1 hr at 1800 C prior to irradiation. These specimens were irradiated to uranium burnups of 0.004 and 0.016 a/o, as determined by dosimetry, at temperatures of about 150 C (Table 9). After these low-temperature short-term irradiations, no apparent physical damage was

TABLE 9. CONDITIONS FOR URANIUM CARBIDE IRRADIATIONS

Capsule	Specimen[a]	Nominal Carbon Content, w/o	Preirradiation Heat Treatment		Effective Thermal-Neutron Flux (From Dosimetry), 10^{13} nv	Specimen-Surface Temperature Range, C	Total Uranium Burnup, a/o	
			Temperature, C	Time, hr			By Isotopic Analysis	By Dosimetry
BRR-1	2T	5.0	1800	1	--	150	--	--
	2B	5.0	1800	1	--	150	--	--
	9T	5.0	1800	1	1.01	150	--	0.004
	9B	5.0	1800	1	1.01	150	--	0.004
	11B	5.0	1800	1	--	150	--	--
	15T	5.0	1800	1	--	150	--	--
BRR-2	7T	5.0	1800	1	--	150	--	--
	7B	5.0	1800	1	--	150	--	--
	11T	5.0	1800	1	1.30	150	--	0.016
	14T	5.0	1800	1	1.30	150	--	0.016
	14B	5.0	1800	1	--	150	--	--
	15B	5.0	1800	1	--	150	--	--
BRR-3	2T′	5.0	1450	5	0.83	150	--	0.28
	1T	5.0	As cast		0.83	150	--	0.28
	5T	5.0	1450	5	0.87	150	--	0.30
	4B	5.0	As cast		0.91	150	0.18	0.32
	19T	6.7	1400	15	0.97	150	--	0.33
	20B	6.7	1400	15	1.00	150	0.20	0.35
BRR-5	8T	5.0	1450	5	0.67	430 - 720[b]	--	0.49
	21T	6.7	1400	15	1.02	--	--	0.74
	24T	8.5	1400	15	0.97	600 - 740[c]	--	0.58
	22B	8.5	1400	15	1.12	--	--	0.61
	21B	6.7	1400	15	0.99	--	0.55	0.72
	10T	5.0	1450	5	0.57	--	0.44	0.42
BRR-6	8B	5.0	1450	5	1.00	490 - 740[b]	--	0.72
	17T	5.0	As cast		0.98	--	--	0.71
	10B	5.0	1450	5	1.06	680 - 810[c]	--	0.76
	16T	5.0	As cast		0.78	--	0.50	0.57
	11T′	5.0	1450	5	0.83	--	--	0.61
	17B	5.0	As cast		0.91	--	0.44	0.66

(a) Specimens 2T′ and 11T′ duplicate Specimens 2T and 11T except that they were prepared from 10 per cent enriched rather than natural uranium.

(b) During Cycle 68, surface temperatures may have reached 870 C.

(c) During Cycle 68, surface temperatures may have reached 980 C.

observed in any of the specimens (Figure 12). The measurements of physical dimensions performed after irradiation failed to reveal any gross changes and the decreases of the fuel density were in all cases less than 1 per cent, see Table 10. The microstructural studies performed both before and after irradiation by both optical and electron microscopic techniques failed to reveal any changes in either the uranium monocarbide or the second-phase uranium dicarbide. However, the measurements of electrical resistivity, which showed a major increase after the short-term low-temperature irradiation exposures (Table 11), suggested that saturation of displaced interstitials and vacancies in the lattice was attained. The measurements of irradiation-induced lattice-parameter changes by X-ray diffraction studies showed that an expansion in the uranium monocarbide lattice had occurred and, like the electrical resistivity, approached an upper limit after the short-term irradiation exposures (Table 12).

The uranium-5.0 w/o carbon specimens which were irradiated in Capsules BRR-3 and BRR-4 were fabricated from 10 per cent enriched uranium. The specimens in Capsule BRR-3 were irradiated to average uranium burnups of about 0.17 a/o at temperatures of about 150 C (Table 9). During irradiation, fission gases were detected escaping from Capsule BRR-4, necessitating its immediate discharge from the reactor. During the postirradiation examination of this capsule, a portion of the inner capsule shell was found to have melted. The uranium carbide specimens were completely disintegrated. This capsule failure is believed to have been brought about by a separation of the helium-argon mixture used in the gas annulus of this capsule.

The specimens in Capsule BRR-3 were found to be apparently unaffected by irradiation. A typical specimen is shown in Figure 13. Like the specimens from the first two capsules, only minor dimensional changes were measured, and the density decreases were no more than 1 per cent (Table 10). The optical and electron microscopy examinations revealed essentially no changes in the microstructures of the as-cast specimens or in those heat treated prior to irradiation. Figure 14 shows the typical structure of this fuel material after being irradiated to about 0.18 a/o uranium burnup. The electron microscopy examinations did reveal regions of fine markings adjacent to the UC_2 platelets, as shown in Figure 15 corresponding to possible disorder. The measurements of electrical resistivity showed increases quite similar to those observed in the specimens from Capsules BRR-1 and BRR-2 (Table 11). Measurements of lattice parameters in these specimens also indicated that the amount of lattice expansion had not appreciably changed as compared to the specimens irradiated to very low burnups at similar temperatures. Some slight increase in elastic strain was observed (Table 12, Specimens 2T′ and 4B).

The 10 per cent enriched uranium-5.0 w/o carbon specimens contained in Capsules BRR-5 and BRR-6 were irradiated to uranium burnups of about 0.5 a/o at temperatures ranging from 430 C to possibly as high as 980 C (Table 9). These specimens in all cases appeared to be in good condition, showing no evidence of physical damage. A typical specimen is shown in Figure 16. Changes in the physical dimensions of these specimens were found to be no more than 1 per cent and the decreases in density after irradiation were measured in some cases to be slightly in excess of 1 per cent (Table 10). The decreases in density for these high-temperature high-burnup specimens ranged from about 0.8 to 2.7 per cent per a/o uranium burnup. These changes are comparable to decreases of about 1.0 to 1.6 per cent per a/o burnup observed in specimens irradiated to higher burnups and at slightly lower temperatures

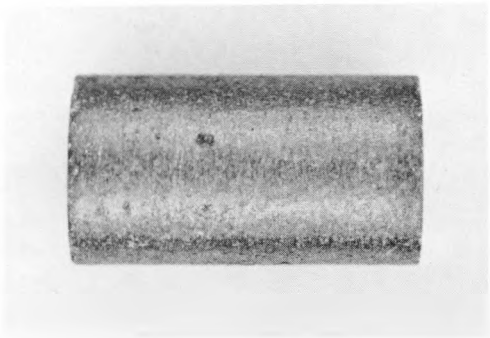

4X RM15655

4X RM15635

a. Before Irradiation

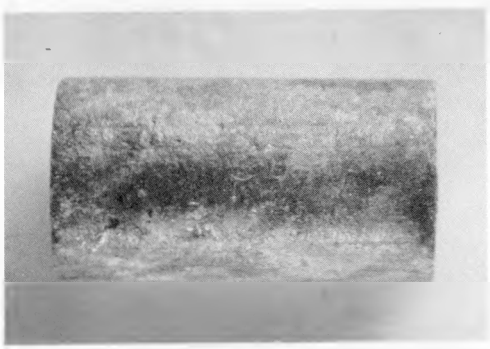

4X HC5484

4X HC5483

b. After Irradiation

FIGURE 12. URANIUM-5 w/o CARBON SPECIMEN BEFORE AND AFTER IRRADIATION TO A URANIUM BURNUP OF 0.004 a/o AT A TEMPERATURE OF 150 C

Specimen 15T, which is typical of those irradiated in Capsules BRR-1 and BRR-2, is shown here.

TABLE 10. CHANGES IN PHYSICAL DIMENSIONS OF IRRADIATED URANIUM CARBIDE SPECIMENS

Capsule	Specimen	Nominal Carbon Content, w/o	Preirradiation Dimensions		Postirradiation Dimensions		Dimensional Changes, per cent	
			Diameter, in.	Density, g per cm^3	Diameter, in.	Density, g per cm^3	Diameter	Density
BRR-1	2T	5.0	0.2505	13.46	0.2510	13.39	+0.2	-0.5
	2B	5.0	0.2506	13.32	0.2512	13.38	+0.2	+0.5
	9T	5.0	0.2501	13.44	0.2507	13.39	+0.2	-0.3
	9B	5.0	0.2501	13.45	0.2506	13.45	+0.2	--
	11B	5.0	0.2503	13.50	0.2502	13.38	--	-0.9
	15T	5.0	0.2503	13.37	0.2503	13.33	--	-0.3
BRR-2	7T	5.0	0.2509	13.52	0.2510	13.47	--	-0.4
	7B	5.0	0.2510	13.50	0.2515	13.48	+0.2	-0.2
	11T	5.0	0.2503	13.50	0.2510	13.44	+0.3	-0.5
	14T	5.0	0.2510	13.36	0.2516	13.32	+0.2	-0.3
	14B	5.0	0.2507	13.36	0.2512	13.32	+0.2	-0.3
	15B	5.0	0.2502	13.37	0.2508	13.32	+0.2	-0.4
BRR-3	2T′	5.0	0.2497	13.43	0.2498	13.44	--	+0.1
	1T	5.0	0.2500	13.40	0.2504	13.30	+0.2	-0.7
	5T	5.0	0.2498	13.54	0.2500	13.41	+0.1	-1.0
	4B	5.0	0.2499	13.34	0.2502	13.36	--	+0.1
	19T	6.7	0.2502	12.62	0.2494	12.72	-0.3	+0.8
	20B	6.7	0.2501	12.63	0.2498	12.76	--	+1.0
BRR-5	8T	5.0	0.2504	13.52	0.2502	13.35	--	-1.2
	21T	6.7	0.2503	12.63	0.2478	12.79	-1.0	+1.3
	10T	5.0	0.2502	13.42	0.2525	13.26	+0.9	1.2
BRR-6	8B	5.0	0.2508	13.52	0.2494	13.36	-0.6	-1.2
	17T	5.0	0.2501	13.47	0.2499	13.37	--	-0.7
	10B	5.0	0.2502	13.41	0.2496	13.34	-0.2	-0.6
	16T	5.0	0.2497	13.49	0.2503	13.37	+0.2	-0.9
	11T′	5.0	0.2500	13.38	0.2498	13.34	--	-0.3
	17B	5.0	0.2509	13.49	0.2504	13.38	-0.2	-0.7

TABLE 11. CHANGES IN THE ELECTRICAL RESISTIVITY OF URANIUM CARBIDE AS A RESULT OF IRRADIATION

Capsule	Specimen	Nominal Carbon Content, w/o	Electrical Resistivity		Increase, per cent
			Before Irradiation, microhm-cm	After Irradiation, microhm-cm	
BRR-1	2T	5.0	36	91	153
	2B	5.0	33	95	187
	9T	5.0	32	--	--
	9B	5.0	32	88	175
	11B	5.0	35	95	172
	15T	5.0	36	--	--
BRR-2	7T	5.0	32	91	184
	7B	5.0	30	97	210
	11T	5.0	35	--	--
	14T	5.0	37	101	173
	14B	5.0	33	87	164
	15B	5.0	34	96	183
BRR-3	2T′	5.0	37	157	325
	1T	5.0	38	108	184
	5T	5.0	37	90	144
	4B	5.0	37	85	130
	19T	6.7	50	211	323
	20B	6.7	48	265	453
BRR-5	8T	5.0	38	59	55
	21T	6.7	48	406	745
	10T	5.0	37	--	--
BRR-6	8B	5.0	37	47	27
	17T	5.0	37	49	32
	10B	5.0	38	67	76
	16T	5.0	34	53	56
	11T′	5.0	35	57	63
	17B	5.0	36	55	53

TABLE 12. CHANGES OF UC LATTICE PARAMETERS AS A FUNCTION OF TEMPERATURE AND BURNUP AS INDICATED BY X-RAY DIFFRACTION STUDIES AND ELECTRICAL RESISTIVITY MEASUREMENTS

Specimen	Nominal Carbon Content, w/o	Average Irradiation Temperature, C	Total Uranium Burnup, a/o	Average Electrical Resistivity, microhm-cm		Lattice Expansion, $\Delta a/a$	Elastic RMS Strain, per cent
				Before	After		
9T	5.0	~150	0.004[a]	32	90(est.)	0.14	0.14
11T	5.0	~150	0.016[a]	35	94(est.)	0.15	0.17
2T′	5.0	~150	0.15[b]	37	157	0.14	0.20
4B	5.0	~150	0.18	37	85	0.19	0.28
20B	6.7	~150	0.20	48	265	0.16[c]	0.38[c]
8T	5.0	430 - 720	0.47[b]	38	59	0.1	0.45
21T	6.7	600 - 740	0.56[b]	48	406	--[d]	0.37[c]
10B	5.0	680 - 810	0.66[b]	38	67	0.2	0.21

(a) Uranium burnups calculated from results of dosimetry analyses.

(b) Estimated burnups from dosimetry analysis and isotopic analyses performed on other specimens in the same capsule.

(c) Measurements from the UC second phase in the U_2C_3 matrix.

(d) Because of the higher burnup and higher radioactivity of this specimen it was not possible to prepare a sufficiently large sample of powder for examination of the second phase (UC).

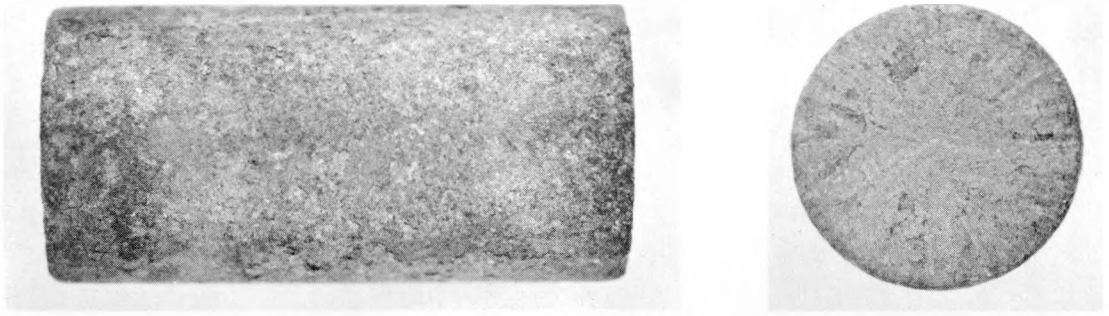

6X RM16961 6X RM16985

a. Before Irradiation

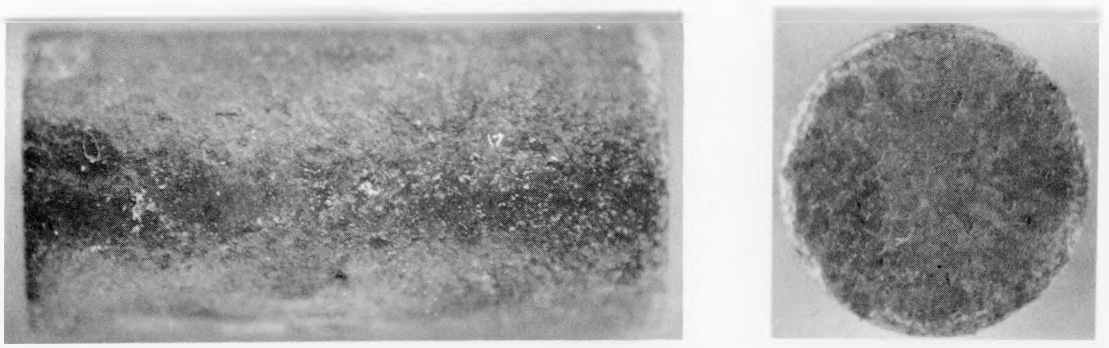

6X HC7021 6X HC7022

b. After Irradiation

FIGURE 13. TYPICAL URANIUM-5.0 w/o CARBON SPECIMEN AFTER IRRADIATION AT 150 C TO A URANIUM BURNUP OF 0.15 a/o

Specimen 2T′ from Capsule BRR-3 is shown here.

100X HC7153

FIGURE 14. TYPICAL MICROSTRUCTURE OF URANIUM-5.0 w/o CARBON SPECIMEN AFTER IRRADIATION AT 150 C TO A URANIUM BURNUP OF 0.15 a/o

Specimen 1T from Capsule BRR-3 is shown.

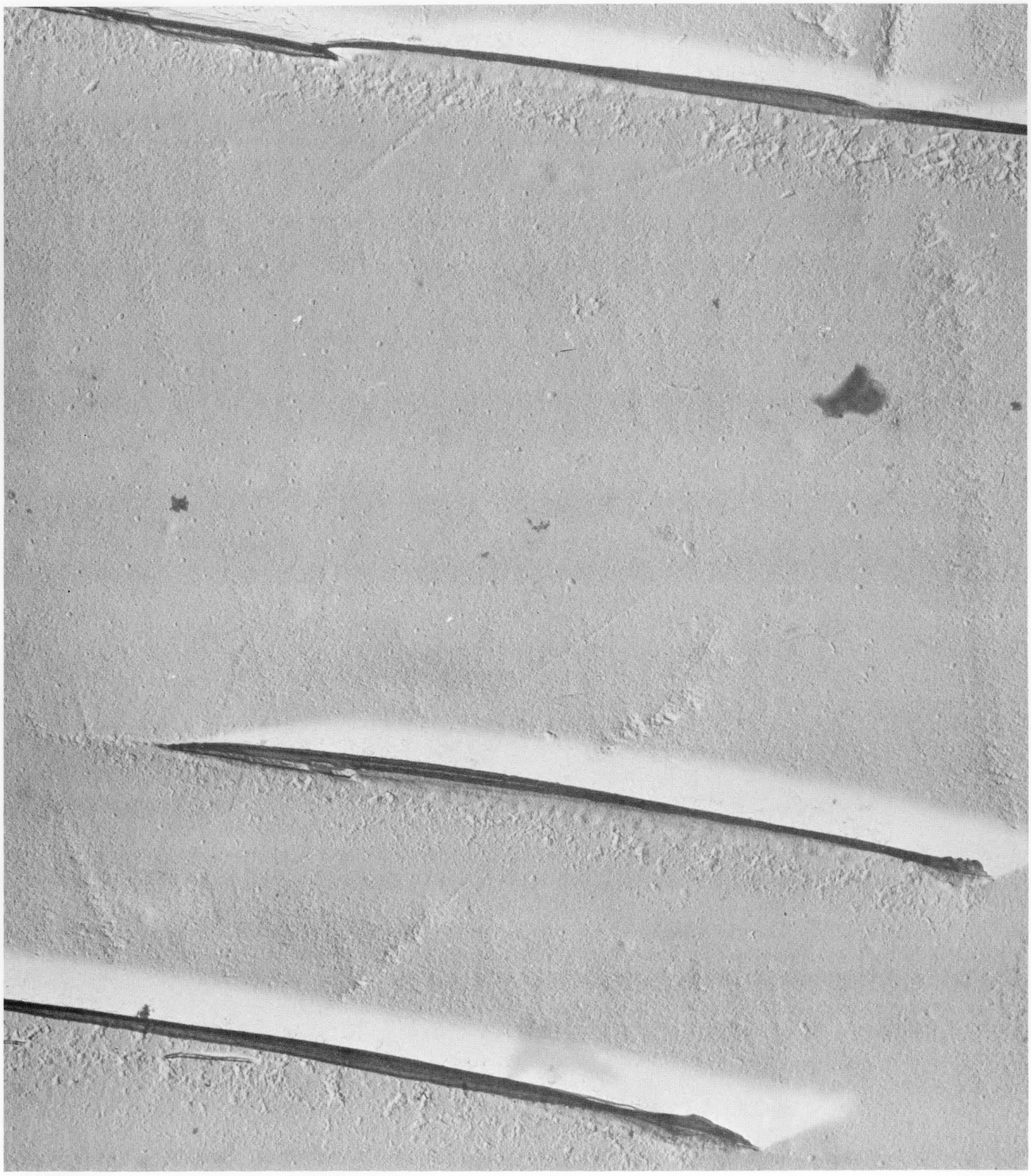

17,500X J2265

FIGURE 15. ELECTRON MICROGRAPH OF SPECIMEN 5T FROM CAPSULE BRR-3 SHOWING REGIONS OF UNIDENTIFIED FINE MARKINGS ADJACENT TO UC_2 PLATELETS

This specimen was heat treated at 1450 C for 5 hr prior to irradiation. The very dark needles are a result of flaps in the replica which occurred along the UC_2 platelets.

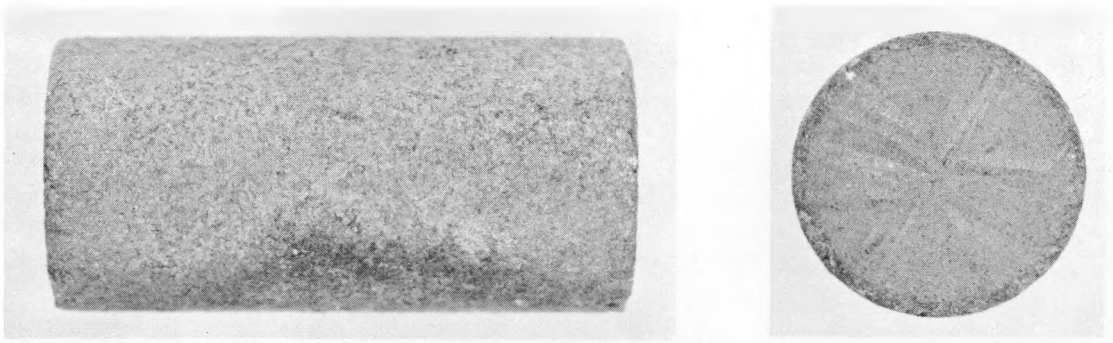

6X RM16978 6X RM17002

a. Before Irradiation

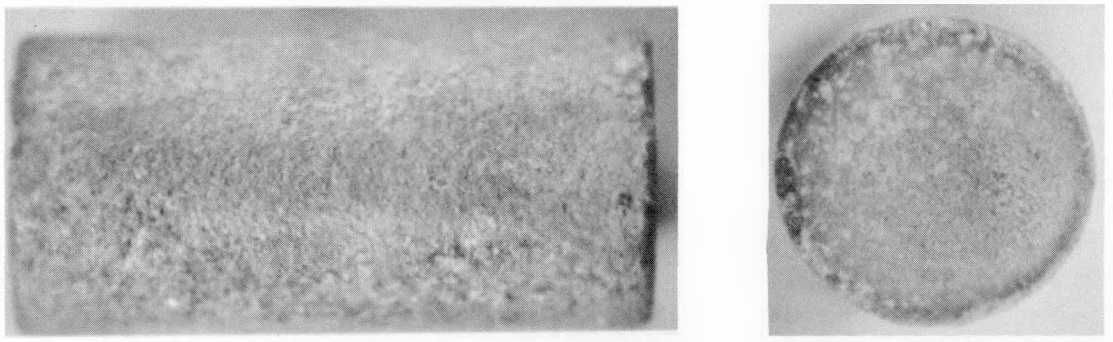

6X HC7845 6X HC7846

b. After Irradiation

FIGURE 16. URANIUM-5.0 w/o CARBON SPECIMEN IRRADIATED AT 490 TO 740 C TO A URANIUM BURNUP OF ABOUT 0.48 a/o

Specimen 8B from Capsule BRR-6 is shown here.

in earlier irradiation studies.[4,5] Microstructural examination of representative specimens from these capsules showed that a depletion of the carbon-rich second phase in a narrow band around the outer circumference of each specimen had occurred (Figure 17). Also, some evidence of surface deterioration was observed in the specimens (Figure 17a). However, since this condition had at times been detected in specimens after fabrication, (Figure 18), and since special precautions had been taken prior to irradiation to reduce the oxygen content of the NaK, it is believed that this surface condition may have existed prior to encapsulation.

One specimen from Capsule BRR-5 showed a typical second phase of U_2C_3 rather than UC_2 (Figure 19). This condition is not believed to have been brought about during irradiation but was caused by the preirradiation heat treatment of 5 hr at 1450 C.

Complete depletion of the UC_2 second phase was observed in a microstructure obtained from one as-cast specimen from Capsule BRR-6 (Figure 20). Although the second-phase depletion appeared complete in this specimen, it is probable that this metallographic section was obtained near an outer surface where the depletion would have been similar to that shown near the outer surfaces in Figure 17. Unfortunately, this specimen decomposed, thereby preventing further grinding and examination.

Difficulty was encountered in obtaining replicas for electron microscopic examinations from the specimens from Capsules BRR-5 and BRR-6. The radioactivity of the replicas was too high to permit examination in the electron microscope, and these studies were abandoned.

Fission-gas-release measurements on Capsule BRR-6, which contained uranium-5.0 w/o carbon alloys, showed that a release of only 0.3 per cent had occurred. This amount is about 2.5 times greater than that which have been expected from surface recoil.

Specimens irradiated at the higher temperatures in Capsules BRR-5 and BRR-6 showed only modest increases of resistivity as compared to the increase observed in the specimens irradiated at lower temperatures (Table 11). The average increase in the electrical resistivity of the specimens irradiated above 600 C was about 52 per cent as compared to an average increase of about 185 per cent for the specimens irradiated at about 150 C. These data indicate that an annealing of those irradiation-induced defects which affect conductivity occurred at the higher temperature.

X-ray diffraction data on Specimens 8T and 10B (Capsules BRR-5 and BRR-6) revealed that the lattice expansion and lattice strain of the UC irradiated above 600 C was essentially the same as measured for the specimens of lower uranium burnup, 0.18 a/o, after irradiation at temperatures of about 150 C (Table 12). The greater elastic strain measured for Specimen 8T may be related to the presence of U_2C_3 in the structure (Figure 19). The lattice expansion in this case was only half of that occurring in a specimen without U_2C_3 in the structure (Figure 17a).

Evaluation of Uranium-6.7 w/o Carbon Alloys

In an effort to make an initial survey of the irradiation stability of the higher carbon content uranium-carbon alloys, two specimens of uranium-6.7 w/o carbon alloy were irradiated in three of the capsules. These studies were designed to examine the

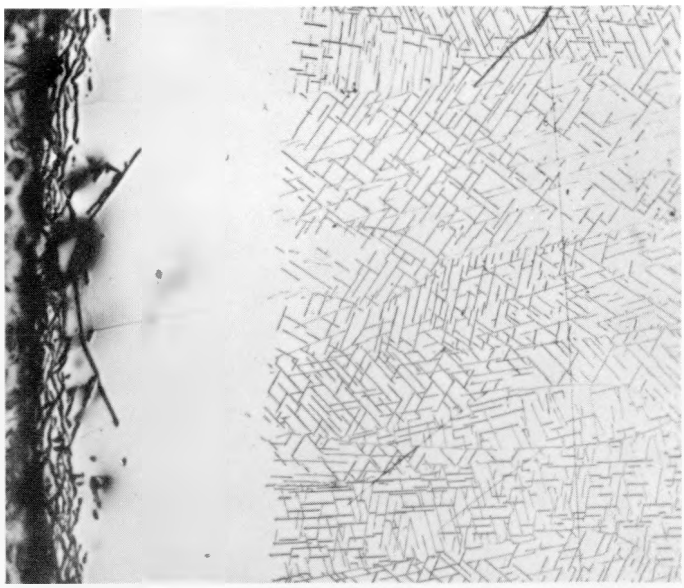

100X HC7902

a. Specimen 10B After Irradiation at 680 to 810 C in Capsule BRR-6 to a Uranium Burnup of About 0.52 a/o

Note depletion of UC_2 second phase at outer edge.

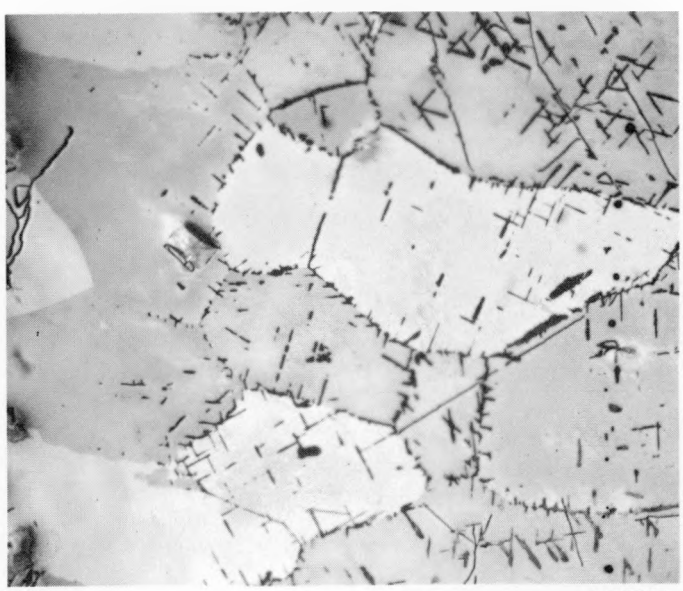

100X HC7875

b. Specimen 8T After Irradiation at 430 to 720 C in Capsule BRR-5 to a Uranium Burnup of About 0.44 a/o

Note depletion of U_2C_3 second phase at outer edge.

FIGURE 17. METALLOGRAPHIC EVIDENCE OF CARBON DEPLETION AT SURFACE IN IRRADIATED URANIUM-5.0 w/o CARBON

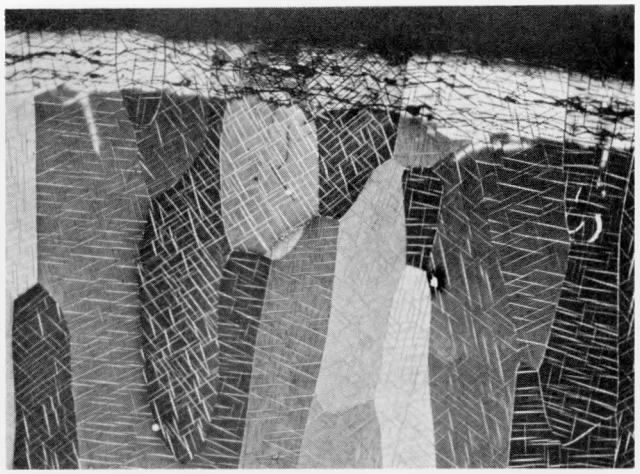

100X RM19483

FIGURE 18. SURFACE CONDITION PRODUCED ON UNIRRADIATED URANIUM MONOCARBIDE AS A RESULT OF ATTACK BY MOISTURE

250X HC7867

FIGURE 19. TYPICAL APPEARANCE OF URANIUM-5.0 w/o CARBON ALLOY AFTER 5-HR HEAT TREATMENT AT 1450 C

The second phase is U_2C_3. Specimen 8T from Capsule BRR-5 is shown here.

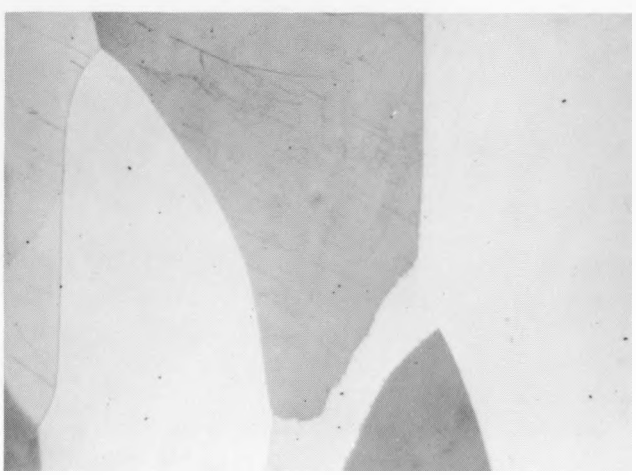

250X HC7912

FIGURE 20. EVIDENCE OF COMPLETE DEPLETION OF UC_2 SECOND PHASE NEAR SURFACE OF URANIUM-5.0 w/o CARBON SPECIMEN IRRADIATED AT 580 TO 770 C TO A URANIUM BURNUP OF ABOUT 0.48 a/o

Specimen 17T from Capsule BRR-6 is shown here.

irradiation behavior of this alloy during irradiations at temperatures of about 150 C and at moderate burnups and at temperatures near 700 C at both moderate and high burnups. However, because of the failure of Capsule BRR-4, the specimens irradiated to a moderate burnup at high temperatures were lost.

The uranium-6.7 w/o carbon-alloy specimens were fabricated from 10 per cent enriched uranium and heat treated for 15 hr at 1400 C before encapsulation to transform the as-cast material to an equilibrium structure of U_2C_3 + UC, as previously mentioned. As was observed for the 5.0 w/o carbon alloys, these specimens generally withstood the irradiations without any major physical damage (Figure 21). Some radial cracking was observed in each of the specimens during the metallographic examinations, and one high-temperature high-burnup specimen was broken extensively on one end. However, since some difficulty was encountered during the removal of this specimen from Capsule BRR-5, it is not known whether or not the breakage occurred during irradiation. The measurements of physical dimensions in all cases showed diametral decreases, 1 per cent and less, accompanied by density increases as great as 1.3 per cent (Table 10). The microstructural studies performed on these specimens by optical techniques failed to reveal any changes resulting from the irradiations (Figure 22). However, the microstructural examinations of the uranium-6.7 w/o carbon specimens after irradiation by replication and electron microscopic techniques revealed a delineation of the grain boundaries of the U_2C_3 phase (Figure 23) which was not observable in electron microscopic examinations of unirradiated specimens prepared by similar etching techniques (Figure 24). The presence of these grain boundaries, however, was revealed in the unirradiated specimen by ordinary metallographic techniques (Figure 22) and by vacuum-cathodic etching techniques (Figure 25). The ease with which these grain boundaries were revealed after a moderate uranium burnup at low temperature may possibly be the result of the segregation of fission products to these boundaries.

The electrical-resistivity measurements performed on the uranium-6.7 w/o carbon specimens showed that large increases in resistivity had occurred after moderate irradiation exposures at low temperatures (Table 11). Unlike the behavior observed for the low-carbon alloy, no annealing of radiation damage during high-temperature exposure was indicated by the resistivity data. Instead, the electrical resistance of the material increased as a function of burnup even at a temperature above 600 C. The X-ray diffraction studies performed on the uranium sesquicarbide (U_2C_3) specimens showed that a lattice contraction occurred during the irradiation to moderate uranium burnups at low temperatures (Table 13). These results are in agreement with the density increases and dimensional decreases measured after irradiation (Table 10). The X-ray diffraction data for the residual uranium monocarbide in these specimens were quite similar to the results obtained for the low-carbon alloy specimens of the low-temperature low-burnup irradiations, (Table 12). The X-ray diffraction results for the uranium sesquicarbide (U_2C_3) exposed to high-temperature high-burnup irradiations showed further lattice contraction as compared to the lower burnup low-temperature data (Table 13). The elastic strain was also found to increase relative to that of the low-burnup material.

6X RM16974 6X RM16998

a. Before Irradiation

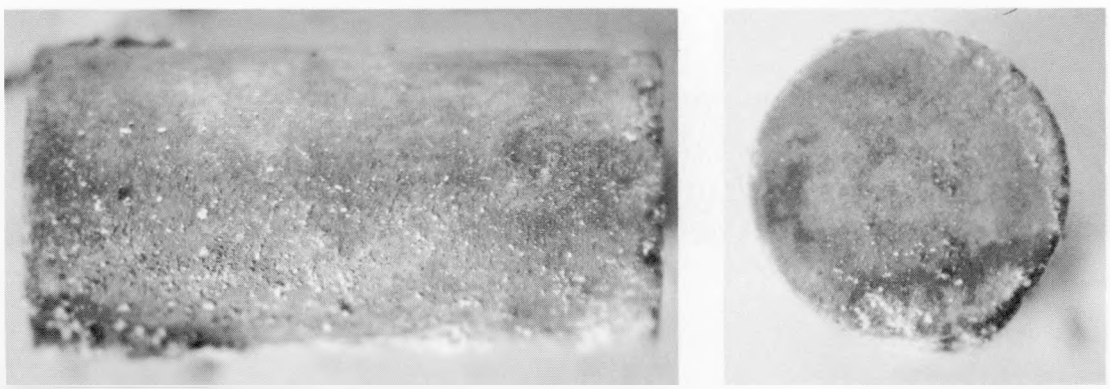

6X HC7863 6X HC7864

b. After Irradiation

FIGURE 21. TYPICAL URANIUM-6.7 w/o CARBON SPECIMEN IRRADIATED AT 540 TO 730 C TO A URANIUM BURNUP OF ABOUT 0.55 a/o

Specimen 21T from Capsule BRR-5 is shown here.

250X RM17221

a. Before Irradiation

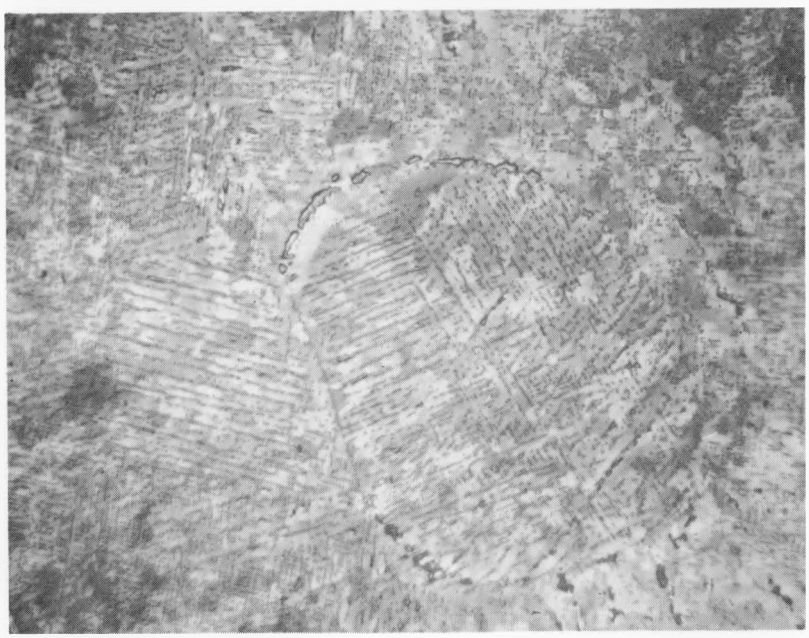

250X HC7883

b. After Irradiation

FIGURE 22. MICROSTRUCTURE OF URANIUM-6.7 w/o CARBON SPECIMEN IRRADIATED AT 540 TO 730 C TO A URANIUM BURNUP OF 0.55 a/o

UC in a matrix of U_2C_3 is evident in this typical sample. Specimen 21T from Capsule BRR-5 is shown.

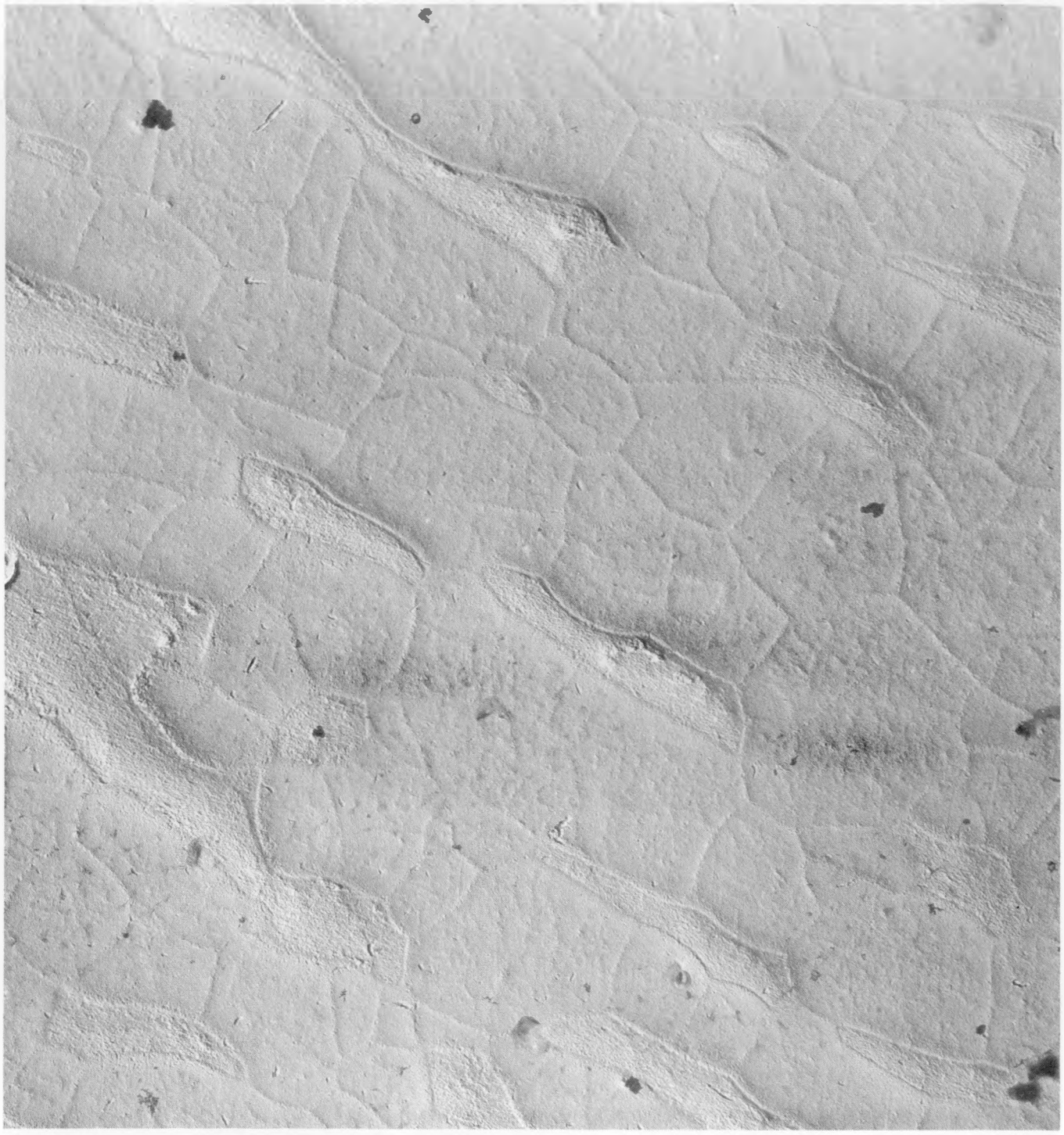

17,500X J2271

FIGURE 23. STRUCTURE OF URANIUM-6.7 w/o CARBON ALLOY CHEMICALLY ETCHED AFTER IRRADIATION

The UC appears as rough-surfaced islands. The matrix with delineated grain structure is U_2C_3. Specimen 19T, irradiated at 150 C in Capsule BRR-3 to a uranium burnup of 0.20 a/o, is shown here.

17,500X J1887

FIGURE 24. STRUCTURE OF URANIUM-6.7 w/o CARBON ALLOY CHEMICALLY ETCHED PRIOR TO IRRADIATION

The UC appears as rough-surfaced islands in smooth matrix of U_2C_3. Compare with Figure 22.

17,500X J2824

FIGURE 25. STRUCTURE OF URANIUM-6.7 w/o CARBON ALLOY ETCHED HEAVILY BY VACUUM-CATHODIC TECHNIQUES

The UC appears as smooth islands of U_2C_3. A grain structure is now evident in the U_2C_3. Compare with Figure 22.

TABLE 13. CHANGES IN THE LATTICE PARAMETERS OF U_2C_3 AS A FUNCTION OF TEMPERATURE AND BURNUP AS INDICATED BY X-RAY DIFFRACTION STUDIES AND ELECTRICAL-RESISTIVITY MEASUREMENTS

Specimen	Nominal Carbon Content, w/o	Average Irradiation Temperature, C	Total Uranium Burnup, a/o	Average Electrical Resistivity, microhm-cm		Lattice Expansion, $\Delta a/a$	Elastic RMS Strain, per cent
				Before	After		
20B	6.7	~150	0.20	48	265	-0.14	0.22
21T	6.7	600 - 760	0.56[a]	48	405	-0.6	0.39

(a) Estimated burnup from dosimetry analysis and isotopic analyses performed on other specimens in the capsule.

Evaluation of Uranium-8.5 w/o Carbon Alloy

Preliminary studies of the irradiation stability of uranium dicarbide were attempted by irradiating two specimens of uranium-8.5 w/o carbon alloy in one of the high-burnup high-temperature capsules. However, during the postirradiation examination of this capsule, these specimens were found to have completely disintegrated during irradiation.

The mechanism of disintegration of these uranium-8.5 w/o carbon alloy specimens cannot be fixed with certainty. Some of the control specimens of this composition heated for 15 hr at 1400 C had the structure shown in Figure 26a; others had the structure shown in Figure 26b. Since graphite is known to be attacked by NaK(8) the presence of free graphite in the irradiation specimens could easily account for the disintegration of these uranium-8.5 w/o carbon specimens irradiated in Capsule BRR-5.

To examine this possibility, three of the uranium-8.5 w/o carbon alloy control specimens for this irradiation which had been heat treated for 15 hr at 1400 C were re-examined. All contained some graphite as in Figure 26b. These were heated in a NaK capsule for 10 hr at 870 C. All completely disintegrated after 10 hr. An as-cast specimen of uranium-8.5 w/o carbon alloy having the structure shown in Figure 26a survived a similar 100-hr treatment in NaK essentially intact. The structure of the as-cast specimen after this treatment is shown in Figure 27.

Discussion and Conclusions

These radiation-stability studies indicate that uranium monocarbide has excellent resistance to damage by irradiation up to uranium burnups of 0.7 a/o at temperatures up to 980 C. As was observed in earlier irradiation studies(4,5) this fuel alloy was found to withstand irradiation to uranium burnups of 2.8 a/o at about 500 C without any adverse physical property changes.

Measurements of electrical resistivity of specimens irradiated at low temperatures, about 150 C, showed major increases at burnups of 0.004 a/o of the uranium and only a very low rate of increase with continued burnup (Figure 28). These data suggest that a saturation of displaced interstitials and vacancies which may affect the

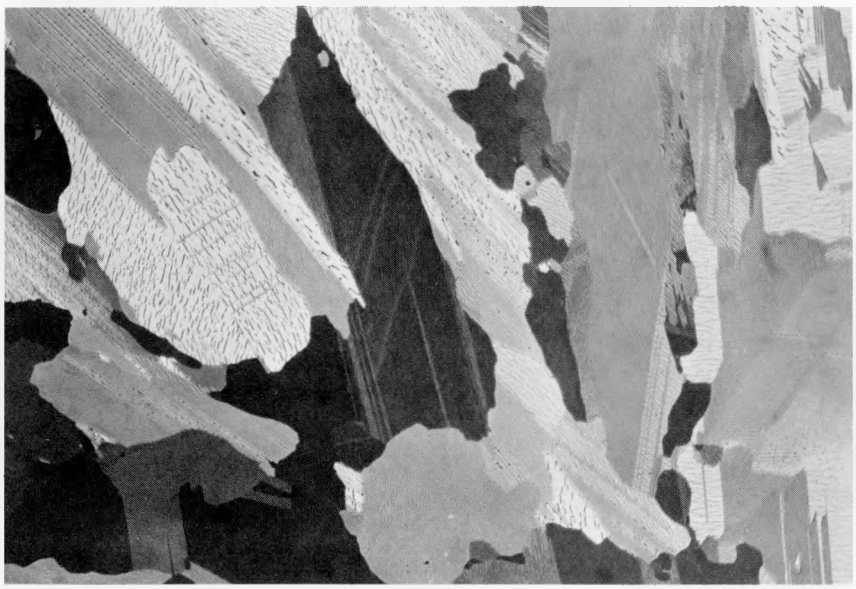

100X Etched RM17226

a. Tetragonal UC_2 Plus Traces of UC

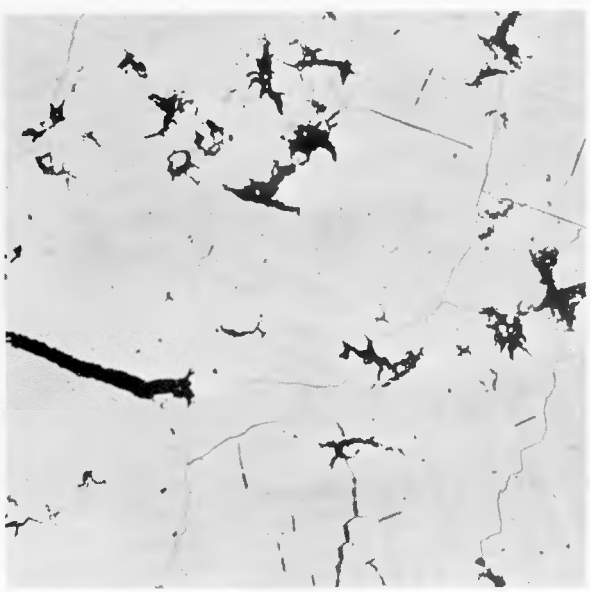

250X As Polished RM19622

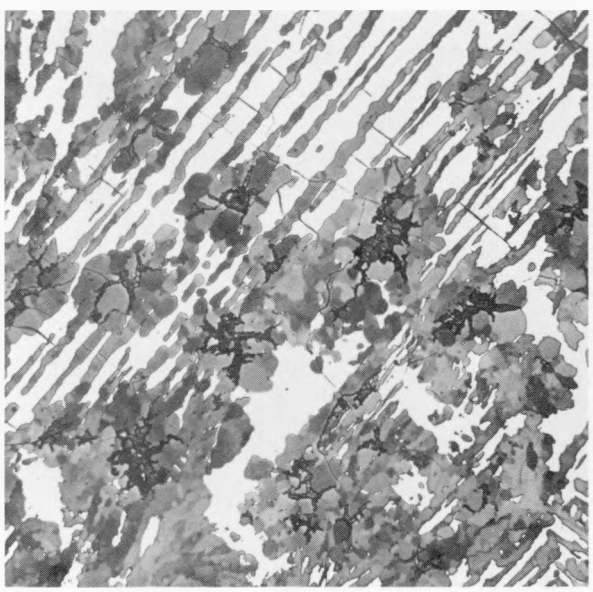

250X Etched RM16923

b. Graphite Surrounded by Dark Dray U_2C_3 and Some Residual UC_2 (White)

FIGURE 26. MICROSTRUCTURES OBSERVED IN THE URANIUM-8.5 w/o CARBON ALLOY AFTER 15-HR HEAT TREATMENT AT 1400 C

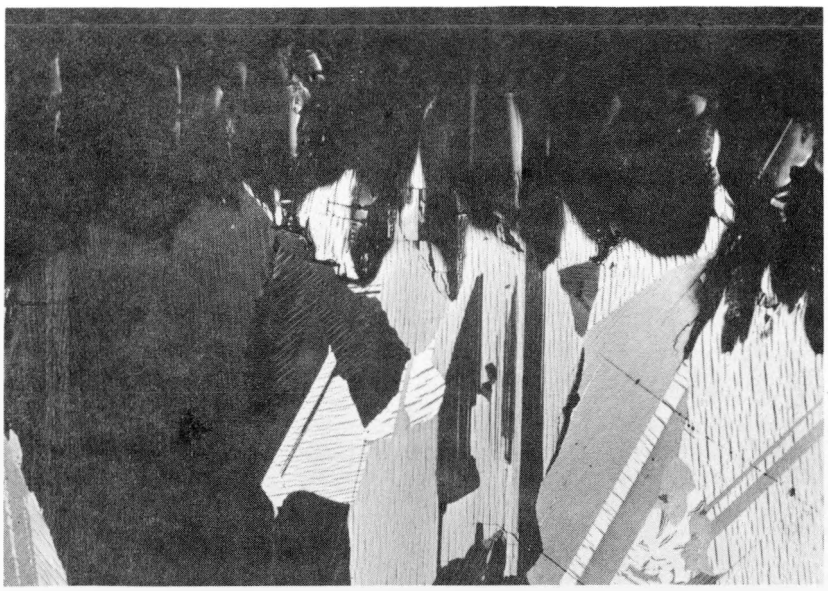

100X Etched RM19801

a. Structure at Edge

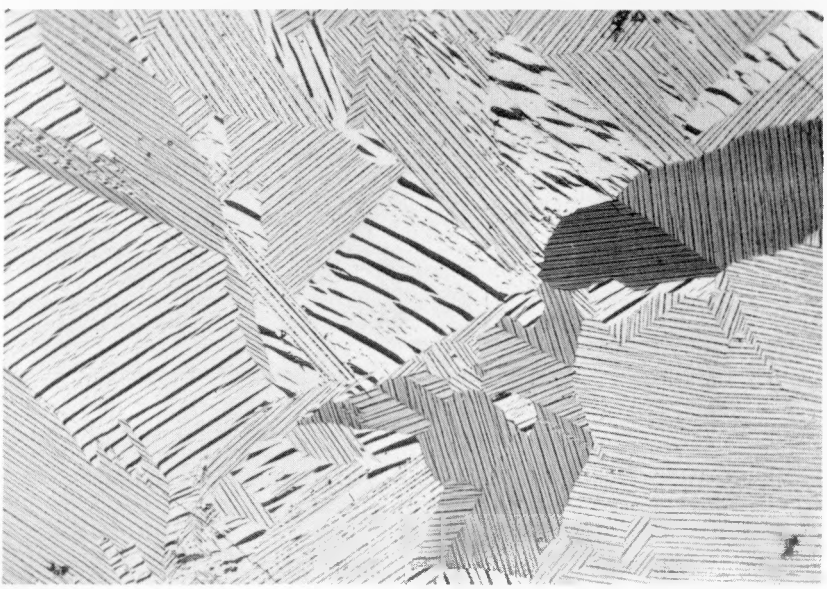

100X Etched RM19804

b. Structure Near Center

FIGURE 27. MICROSTRUCTURES OF AN AS-CAST URANIUM-8.5 w/o CARBON ALLOY HEATED 100 HR IN 810 C NaK

Heat-treated specimens of this composition which contained free graphite in the microstructure disintegrated in a 10-hr exposure to 870 C NaK.

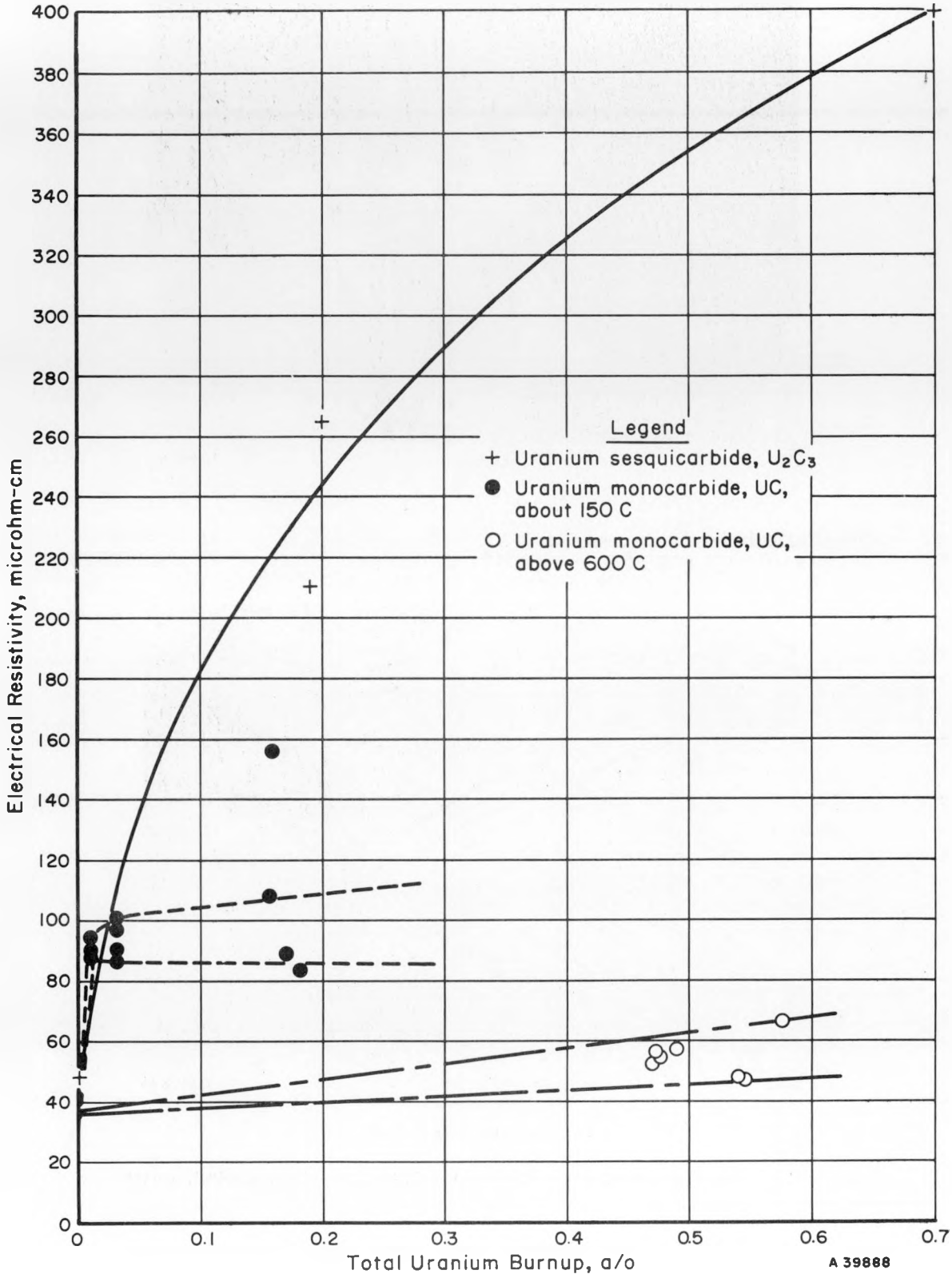

FIGURE 28. CHANGES IN THE ELECTRICAL RESISTIVITY OF UC AND U_2C_3 WITH URANIUM BURNUP

electronic characteristics of the lattice was attained very early during irradiation. The electrical resistivity of the specimens irradiated at high temperatures increased much less than in the case of the specimens irradiated at low temperature, indicating that the damage incurred was annealed out to a large degree during the high-temperature irradiations.

Measurements of irradiation-induced lattice-parameter changes showed that lattice expansion in uranium monocarbide, like the electrical resistivity, approached an upper limit after very short-term exposures, Figure 29. Calculations of the maximum lattice expansion expected as a result of fission-fragment accumulation show that the lattice expansion produced during these short irradiations was not related to the production of fission products. It follows that the expansion must have been caused by displaced interstitials and vacancies in the lattice. However, after this large initial increase of the lattice parameter at low uranium burnups, further lattice expansion at higher burnups and low temperatures tends to approximate that which might be expected from fission-fragment accumulation. Therefore, the generation of additional vacancy-interstitial pairs by fissioning must be negated by an annihilation or recombination mechanism.

The line broadening of the X-ray diffraction patterns of the UC irradiated to 0.004 and to 0.016 a/o burnups indicated that both crystallite fragmentation and lattice strain contributed to the line broadening after 0.016 a/o burnup of the uranium. Although some increases in elastic strain were observed with increasing burnup, the greatly decreased rate of change may be associated with crystallite size reduction.

The X-ray studies performed on uranium sesquicarbide indicate that a progressive contraction of the complex body-centered-cubic lattice of U_2C_3 may be expected with increasing irradiation exposures. The X-ray diffraction data show such a contraction with increased uranium burnups from 0.20 a/o to 0.56 a/o. As indicated by both the electrical-resistivity and X-ray diffraction data, no annealing of the irradiation-induced damage was observed in U_2C_3 at temperatures above 600 C. The lattice contraction and density increase in uranium sesquicarbide during irradiation may possibly be accounted for by substitution of some fission-product atoms for uranium in the structure. This would tend to result in a decreased average metal valency and a shortening of the carbon-carbon band. For instance, the rare-earth sesquicarbides have a carbon-carbon bond distance of 1.236 A as compared to 1.295 A for U_2C_3.[9]

Although the irradiation of bulk uranium dicarbide, uranium-8.5 w/o carbon, resulted in a complete disintegration of the specimens, there is some question as to the mechanism by which this condition resulted. Prior experiments have suggested that UC_2 dispersed in UC decomposes under irradiation at a rate dependent on temperature.[6] A more plausible explanation for the decomposition of the UC_2 specimens is indicated by the studies of the compatibility of UC_2 with NaK at 870 C. These studies show, that if graphite is present in the microstructure of uranium-8.5 w/o carbon alloys, complete disintegration will occur within 10 hr. Similar tests performed on UC_2 in the as-cast condition failed to produce disintegration of this alloy after approximately 100 hr. Free graphite was not observed in the microstructure of one heat-treated control specimen, but free graphite was found in the microstructure of other heat-treated specimens from this same group. Although metallographic examinations were not performed on the heat-treated specimens which were irradiated, it is likely that they contained free graphite prior to irradiation.

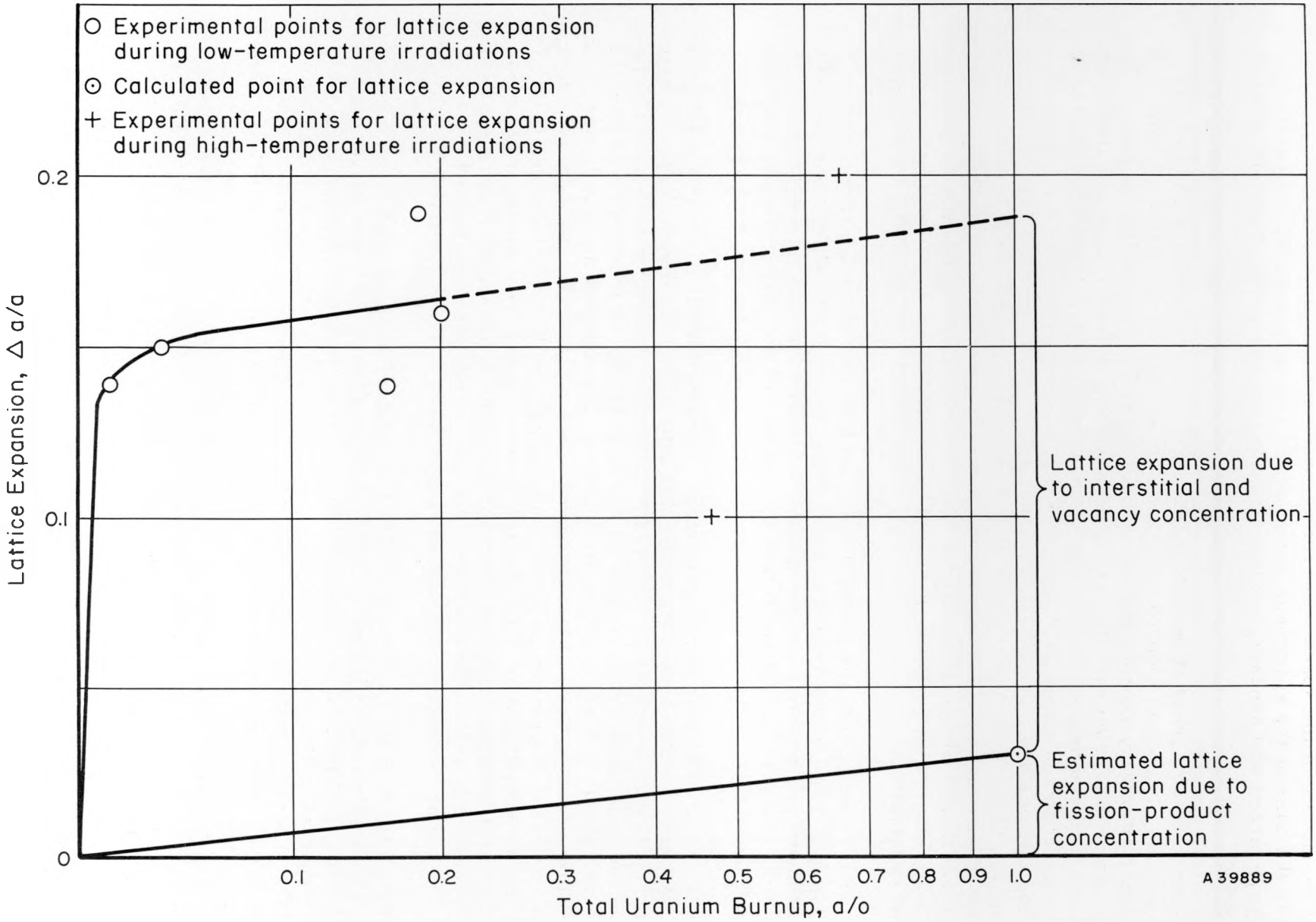

FIGURE 29. THE RELATION OF LATTICE EXPANSION TO URANIUM BURNUP IN URANIUM MONOCARBIDE

DISCUSSION AND EVALUATION

This research demonstrated the technical feasibility of melting and casting of 100 per cent dense uranium carbide ingots weighing up to 6 kg and having controlled carbon contents predictable within plus or minus 0.05 w/o carbon. It was demonstrated that carbide ingots weighing up to 9 kg could be cast into any desired right-cylindrical shape; so it is presumed that the present process could be scaled up at least to this extent with the same degree of compositional control.

Determinations of the physical, mechanical, and chemical properties of uranium carbides at both room and elevated temperatures have confirmed expectations that uranium carbides are suitable fuels for high-temperature nuclear reactors. A major annoying characteristic of uranium carbides is their tendency to react with and deteriorate slowly at room temperature in the presence of water, moist air, or alcohols. Uranium dicarbide has been shown to be metastable at temperatures below about 1400 C; and, as a result, it is not expected to show satisfactory dimensional stability and strength in bulk form in reactor irradiations at high temperatures. Dilation, resistivity, and diffusion data suggest that changes in the structure and properties of metastable uranium dicarbide may begin to occur at about 800 C or 870 C. Diffusion data suggest that reactions of uranium carbide with metals, liquids, and gases will be limited to surface reactions below 800 C. Compatibility of uranium carbide with materials above 800 C will be heavily dependent upon the chemical activity of carbon in the other material.

Hot-hardness data indicate that the creep strength of uranium-carbon alloys will be an important factor in engineering design at temperatures above 1000 C. Diffusion data suggest that the creep strength of unalloyed uranium monocarbide may become so low at about 1300 C that excessive swelling caused by internal fission-gas bubbles may occur.

Changes in the lattice parameters and electrical resistivity of uranium monocarbide as a function of burnup ceased for all practical purposes after a burnup of only 0.01 a/o of the uranium. Samples of uranium monocarbide and uranium sesquicarbide showed no signs of gross distortion or imminent failure after further irradiations to burnups of over 0.5 a/o of the uranium at about 700 C. Samples of uranium dicarbide which had been heat treated to produce some graphite in the structure disintegrated under corrosive attack by NaK during irradiation.

It is concluded that under suitable nonoxidizing conditions uranium monocarbide and uranium sesquicarbide are ideal fuels for power reactors operating at temperatures at least as high as 800 C, and perhaps as high as 1300 C. The utility of uranium dicarbide as a fuel for nuclear reactors is subject to reservations. As a bulk fuel it may have some utility at low temperatures where the rate of graphite formation is negligible. As a fuel dispersed in graphite, the decomposition of metastable uranium dicarbide into uranium sesquicarbide and graphite may not present any serious problems.

These studies have resulted in a basic understanding of the properties and capabilities of the uranium carbides as engineering materials. Much specific developmental work remains to be done. First and foremost among these tasks is the need to define the temperature and burnup limitations of at least uranium monocarbide and uranium sesquicarbide.

Supporting studies on uranium carbides in the areas of alloy development and determination of mechanical properties at high temperatures, conductivity at very high temperatures, and chemical compatibility with materials of reactor construction appear to be most important for the rapid development of these materials as reactor fuels.

REPORTS AND PAPERS ISSUED UNDER THIS PROGRAM

(1) Rough, F. A., and Chubb, W., "Progress on the Development of Uranium Carbide-Type Fuels, Phase I Report on AEC Fuel-Cycle Program", BMI-1370 (August 21, 1959).

(2) Rough, F. A., and Dickerson, R. F., "Uranium Monocarbide – Fuel of the Future?", Nucleonics, 18, 74-77 (March, 1960).

(3) "Progress in Carbide Fuels, Notes From the Second AEC Uranium Carbide Meeting Held at Battelle Memorial Institute, March 22 and 23, 1960", TID-7589 (April 20, 1960).

(4) Rough, F. A., and Chubb, W., "An Evaluation of Data on Nuclear Carbides", BMI-1441 (May 31, 1960).

(5) Phillips, W. M., Chubb, W., and Foster, E. L., "Direct Casting of Uranium Monocarbide Reactor Fuel Elements", J. Less-Common Metals, 2, 451-457 (1960).

(6) Rough, F. A., and Chubb, W., "Progress on the Development of Uranium Carbide-Type Fuels, Phase II Report on the AEC Fuel-Cycle Program", BMI-1488 (December 27, 1960).

(7) Chubb, W., and Rough, F. A., "Research on Uranium Carbide and Uranium Carbide-Base Fuel Materials at Battelle Memorial Institute", Proceedings of the Uranium Carbide Meeting Held at Oak Ridge National Laboratory, December 1-2, 1960, TID-7603, pp 12-24.

(8) Chubb, W., and Phillips, W. M., "Constitution of the Partial System: Uranium Monocarbide-Uranium Dicarbide", Trans. ASM, 53, 465-478 (1961), Discussion, pp 938-939.

(9) Chubb, W., and Dickerson, R. F., "The Properties of Uranium Carbides", J. Am. Ceram. Soc., To be Published.

(10) Freas, D. G., Austin, A. A., and Rough, F. A., "Mechanism of Irradiation Damage in Uranium Monocarbide", ASTM Symposium on Radiation Effects in Refractory Fuel Compounds, June, 1961, To be published.

(11) Keller, D. L., Fackelmann, J. M., Speidel, E. O., and Paprocki, S. J., "Powder Metallurgy of Uranium Carbide and Uranium Nitride", Fourth Plansee Seminar, Reutte/Tyrol, June 20-24, 1961, To be published.

(12) Chubb, W., Townley, C. W., and Getz, R. W., "Diffusion Coefficients of Uranium and Carbon in Uranium Monocarbide", BMI-1551 (November 6, 1961).

REFERENCES

(1) Chubb, W., Townley, C. W., and Getz, R. W., "Diffusion Coefficients of Uranium and Carbon in Uranium Monocarbide", BMI-1551 (November 6, 1961).

(2) Secrest, A. C. Foster, E. L., and Dickerson, R. F., "Preparation and Properties of Uranium Monocarbide Castings", BMI-1309 (January 2, 1959).

(3) Rough, F. A., and Chubb, W., "Progress on the Development of Uranium Carbide-Type Fuels, Phase II Report on AEC Fuel-Cycle Program", BMI-1488 (December 27, 1960).

(4) Hare, A. W., and Rough, F. A., "Irradiation Effects on Massive Uranium Monocarbide", BMI-1452 (July 21, 1960).

(5) Hare, A. W., and Rough, F. A., "The Effect of High-Burnup Irradiation on Massive Uranium Carbide", BMI-1491 (January 6, 1961).

(6) Freas, D. G., Austin, A. E., and Rough, F. A., "Mechanisms of Irradiation Damage in Uranium Monocarbide", ASTM Symposium, Atlantic City, New Jersey (June, 1961).

(7) Power Reactor Technology, Section VIII, "Fuel Elements" (December, 1960).

(8) Liquid Metals Handbook, Third Edition of "Sodium-NaK Supplement" (June, 1955).

(9) Atoji, M., ACA Meeting at Boulder, Colorado (August 4, 1961).